Dissertation

submitted to the

Combined Faculty of Natural Sciences and Mathematics

of the Ruperto Carola University Heidelberg, Germany

For the degree of

Doctor of Natural Sciences

presented by

Master of Science, Yingxue Yang

Born in: Baoji, China

Oral examination: 12.09.2018

Post-translational regulation of redox-sensitive glutamylcysteine ligase (GCL) - revisited

Referees: Prof. Dr. Thomas Rausch

Prof. Dr. Rüdiger Hell

Summary

Glutathione (GSH) has been reported for its crucial roles in maintaining plant growth as well as responding to environmental stresses. The multiple functions of glutathione require a tight control of GSH levels. Glutamylcysteine ligase (GCL) catalyzes the first rate-limiting step of glutathione biosynthesis. However, the mechanism of redox-dependent regulation on GCL is still largely unknown in plants.

Previous findings have demonstrated that formation of an intramolecular disulfide bond followed by homodimerization is unique to the redox-mediated activation of plant GCL. To address whether the disulfide bond formation is sufficient for GCL activation or the subsequent homodimerization is a necessary step, we generated recombinant mutated GCLs unable to form dimers. Enzyme activity assays showed that disrupting dimer formation did not prevent redox-activation of GCL. Substrate affinities were similar among recombinant GCL variants. The dissociation constant of GCL was estimated by FPLC analysis to be less than 10^{-6} M; additionally, the GCL concentration in plastids was estimated to be approximately 5 mM. Therefore, the GCL dimer is likely to occur *in vivo*. Taken together, this study reveals that GCL activation relies primarily on intramolecular disulfide bridge whereas dimerization has little contribution. Whether dimerization affects other enzyme properties, e.g. GCL stability *in vivo*, remains to be investigated.

Mitogen-activated protein kinase (MAPK) cascades mediate signal transduction of diverse extracellular stimuli including pathogen attack and oxidative stress. *Arabidopsis* MAPK3 and MAPK6 can be deactivated by MAPK phosphatase2 (MKP2) which may be involved in oxidative stress-related responses. Therefore, the MKP2-inducible transgenic *Arabidopsis* lines were used to explore the redox dependency of MKP2 regulation. After induction, an attenuated MKP2 accumulation was observed under sustained oxidative stress conditions. MKP2 may act as a potential target for plants to perceive oxidative stress and enhance MAPK signaling. It is conceivable that the post-translational modification of MKP2 exerts such regulation.

Zusammenfassung

Glutathion (GSH), ein Antioxidans, hat eine zentrale Rolle bei der Unterstützung des Pflanzenwachstums sowie der pflanzlichen Reaktion auf Umweltbelastungen. Die vielschichtigen Aufgaben von Glutathion erfordern eine strenge Regulierung des GSH-Spiegels. Das Enzym Glutamylcystein-Ligase (GCL) katalysiert den ersten, geschwindigkeitsbestimmenden Schritt der Glutathion-Biosynthese. Für die Redoxregulation von GCL in Pflanzen gibt es jedoch bisher nur wenige Erkenntnisse.

Bisherige Ergebnisse zeigen, dass die Bildung einer intramolekularen Disulfidbindung gefolgt von einer Homodimerisierung einzigartig für eine Redox-vermittelte Aktivierung der pflanzlichen GCL ist. Um festzustellen, ob die Disulfidbrückenbildung für die GCL-Aktivierung ausreichend ist oder die nachfolgende Homodimerisierung erforderlich ist, wurden rekombinante mutierte Formen der GCL hergestellt, die keine Dimere bilden können. Enzymaktivitätsassays zeigen, dass die Störung der Dimerbildung die GCL-Aktivität nicht beeinflusst und die Substrataffinitäten unter den rekombinanten GCL-Varianten ähnlich sind. Die Dissoziationskonstante von GCL wurde durch FPLC-Analyse auf weniger als 10^{-6} M bestimmt. Zusätzlich wird die GCL-Konzentration in Plastiden auf etwa 5 mM geschätzt. Es ist deswegen davon auszugehen, dass das GCL-Dimere *in vivo* auftreten. Ein Hauptergebnis dieser Studie ist, dass die GCL-Aktivierung größtenteils auf intramolekularen Disulfidbrücken beruht, während die intermolekulare Dimerisierung wenig zur Aktivität beiträgt. Ob die Dimerisierung andere Enzymeigenschaften beeinflußt, z. B. die GCL-Stabilität *in vivo,* muss noch untersucht werden.

Mitogen-aktivierte Proteinkinase (MAPK) - Kaskaden vermitteln die Signaltransduktion verschiedener extrazellulärer Stimuli, einschließlich

Pathogenbefall und oxidativem Stress. Arabidopsis MAPK3 und MAPK6 können durch MAPK-Phosphatase 2 (MKP2) deaktiviert werden. MKP2 scheint an Reaktionen auf oxidativen Stress beteiligt zu sein. Auf Grund dieser Erkenntnisse wurden MKP2-induzierbaren transgenen Arabidopsis-Linien verwendet, um die Redoxabhängigkeit der MKP2-Regulation zu untersuchen. Wie in den Ergebnissen gezeigt wurde, wurde nach Induktion eine abgeschwächte Akkumulation von MKP2 unter anhaltenden oxidativen Stressbedingungen beobachtet. MKP2 könnte eine Option für Pflanzen sein, um oxidativen Stress wahrzunehmen und den MAPK-Signalweg zu verbessern. Es ist denkbar, dass die posttranslationale Modifikation von MKP2 eine solche Regulation ausübt.

1. Introduction

The tripeptide glutathione, γ-glutamyl cysteinyl glycine, is one of the most ubiquitous thiols in eukaryotic cells. It functions in various metabolism and stress responses and acts as an antioxidant against reactive oxygen species and peroxidases via the ascorbate-glutathione cycle (Milla *et al.*, 2003). Glutathione can also detoxify heavy metals and other stress factors (Foyer and Noctor, 2005). In addition, glutathione controls protein redox state by glutathionylation, it interacts with cysteine residues and disulfide bridges within protein spontaneously or *via* glutaredoxins. In plants, the reduced GSH is the major form of glutathione whereas the oxidized GSSG remains at relatively low level. Glutathione synthesis and/or degradation control(s) the balance between GSH and GSSG which is crucial for maintaining the cellular redox state (Meister, 1995).

1.1. Glutathione biosynthesis

Glutathione is synthesized in two ATP-dependent steps:

1. L-glutamate + L-cysteine + ATP → γ-glutamyl-L-cysteine + ADP + Pi

2. γ-glutamyl-L-cysteine + L-glycine + ATP → GSH + ADP + Pi

Glutamylcysteine ligase (GCL) catalyzes the formation of gamma-glutamylcysteine (γ-EC) from glutamate and cysteine. This first reaction is considered as the rate-limiting step for glutathione biosynthesis. Then glutathione synthetase (GS) catalyzes the addition of a glycine residue to yield the tripeptide GSH. In *Arabidopsis*, transcript analysis suggests that GCL is only found in plastids while GS is located in both plastids and cytosol (Wachter *et al.*, 2005).

1.1.1. Sulfate uptake, reduction and incorporation into cysteine

Sulfur assimilation, as one of the fundamental processes in plants, produces a wide variety of metabolites such as cysteine, glutathione, methionine and vitamin cofactors (Leustek *et al.*, 2000; Mendel and Hänsch, 2002; Saito, 2000). It has been extensively studied in recent years due to its functional significance for plant growth and response to environmental changes. Understanding biochemistry and physiology of sulfur assimilation is of great necessity for food and feed (Beinert, 2000; Giles *et al.*, 2003; Hell *et al.*, 2002; Nikiforova *et al.*, 2006; Noctor *et al.*, 2002; Schürmann and Jacquot, 2000).

Like its counterparts nitrogen (N) and phosphorus (P), sulfur (S) is an abundant macronutrient necessary for all organisms (Giovanelli, 1990; Nikiforova *et al.*, 2004). In higher plants, sulfur is taken up by roots in the form of sulfate (SO_4^{2-}) from soil (Leustek and Saito, 1999). The sulfate transporters (SULTRs) detect the sulfur status and mediate transport of the anion to the plastids of plant cell for subsequent assimilation of inorganic sulfate into a variety of organic S compounds (Davidian and Kopriva, 2010; Kankipati *et al.*, 2015; Leustek *et al.*, 2000; Rouached *et al.*, 2009; Takahashi *et al.*, 2011b). The import of available sulfate is considered to trigger sulfur cycle in the nature, which may suggest its central role in the regulation of the whole sulfur assimilation pathway. In the initial steps, ATP sulfurylase (ATPS) catalyze activation of sulfate by adenylation to adenosine-5′-phosphosulfate (APS) in the presence of ATP. APS is reduced to sulfite by APS reductase (APR) and then to sulfide by a ferredoxin dependent sulfite reductase (SIR) (Leustek *et al.*, 2000). APS is also converted to adenosine 3′-phosphate-5′-phosphosulfate (PAPS) by an APS kinase in an additional reaction, the production of which provides a reservoir for APS (Lee and Leustek, 1998; Lillig *et al.*, 2001). Therefore APS serves as the divergence point for the sulfation pathways and sulfur assimilation (Giordano and Raven, 2014).

Cysteine (Cys) biosynthesis takes place after reduction of sulfate. It involves two

consecutive enzyme reactions catalyzed by serine acetyltransferase (SAT) and O-acetylserine (thiol) lyase (OAS-TL). SAT catalyze O-acetylserine (OAS) formation from acetyl-CoA and serine. In the second step, Cys is synthesized by OAS-TL from OAS and sulfide. SAT and OAS-TL are associated with each other as the cysteine synthase complex (CSC) (Droux *et al.*, 1998; Feldman-Salit *et al.*, 2009). SAT is a key rate-limiting enzyme in Cys biosynthesis and its full activity requires OAS-TL(Wirtz and Droux, 2005; Wirtz and Hell, 2006). Taken together, the assimilation of sulfate undergoes the following four steps: sulfate uptake, activation, reduction as well as synthesis of Cys.

As the first organic reductant of sulfur, Cys plays the central role in regulating different steps in plant metabolism (Takahashi *et al.*, 2011b). It serves as amino-acid for building up proteins and it is the sulfur precursor of various sulfur-containing compounds for plant growth, development, and resistance to stress (Hawkesford, 2012). Among its diverse functions, it is important for integration of Cys as substrate into glutathione. The formation of glutathione is crucial for controlling redox homeostasis for stress defense and enables sulfur circulating in the plant cell (see the following introduction) (Noctor *et al.*, 2002). Cys is also the sulfur precursor for amino acid methionine which can be converted to many other important S-containing compounds, including S-methylmethionine (SMM) and S-Adenosyl methionine (SAM) (Amir *et al.*, 2002). Furthermore, Cys donates sulfur to a range of vitamins (biotin and thiamin) as well as cofactors (Co-A and molybdenum cofactor) (Beinert, 2000; Marquet *et al.*, 2001; Mazid *et al.*, 2011; Mendel and Hänsch, 2002; Wittstock and Halkier, 2002).

1.1.2. Glutamylcysteine ligase (GCL)

The biosynthesis of GSH is controlled at multiple levels, where the GCL activity is a key determinant. Sequence alignment of the GCLs from different species suggests that plant GCLs share extensive sequence similarity with GCLs from α-proteobacteria,

but differ from sequences from the *E. coli* and sequences from non-plant eukaryotes (mammals / yeast / trypanosoma). They define the three families of GCLs (Galant *et al.*, 2011) (Figure 1). Sequence comparisons between families do not show high similarities, e.g., *Arabidopsis thaliana* GCL shares less than 25% amino acid sequence identity with the mammalian, yeast, and bacterial versions of the enzyme (May and Leaver, 1994), even though comparisons within every group uncovered some similarities (Copley and Dhillon, 2002).

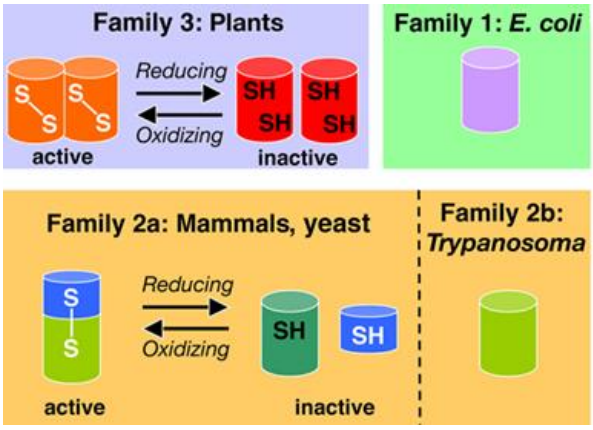

Figure 1. Overview of glutamate–cysteine ligase (Galant *et al.*, 2011)

Oligomeric organization and redox regulation of the three types of GCL are shown.

In addition to the sequence divergence, GCL enzymes from different origins also vary with regard to their structures (Figure 1). In humans and many other eukaryotes, GCL is a heterodimeric enzyme containing two subunits: the catalytic subunit, GCLc and the modulatory subunit, GCLm (Krzywanski *et al.*, 2004). GCLm regulates GCLc activity by formation of holoenzyme complex (Chen *et al.*, 2005; Fraser *et al.*, 2003a). Intermolecular redox-sensitive disulfide bonds mediate reversible formation of GCL heterodimer from two subunits, with activation or inactivation of enzyme in response to redox changes (Fraser *et al.*, 2003b; Tu and Anders, 1998). In contrast, plant GCLs act as homodimeric enzymes under oxidizing condition. The crystallization analysis of GCL from *Brassica juncea* reveals homodimer interface involving a number of amino acid residues (Gromes *et al.*, 2008; Hothorn *et al.*, 2006), as shown in Figure 2. Some salt bridges (E133/R395, E193/K471, E136/N176) and hydrophobic side chains (F135,

Y186, W394, F475) contribute to a zipper-like interface (Gromes *et al.*, 2008; Hothorn *et al.*, 2006). These amino acid residues in the dimer contact zone are highly conserved. There are two disulfide bonds (named CC1 and CC2) within the plant GCL structure. CC1 is located near the active site whereas CC2 is close to homodimer interface (Hothorn *et al.*, 2006) (Figure 2). The sequence alignment revealed that, compared to CC1 which is confined to the rosids clade, CC2 is highly conserved among all the plant species (Gromes *et al.*, 2008). It indicates that CC2 is more crucial for redox regulation than CC1. Formation of intramolecular disulfide bond followed by homodimerization is unique to redox-mediated activation of plant GCL (Gromes *et al.*, 2008). Reducing agents like DTT disconnect activated non-covalently linked GCL dimer interface, changing the conformation from dimer to monomer with reduced (-80%) enzyme activity in a process that can be reversed by re-oxidizing.

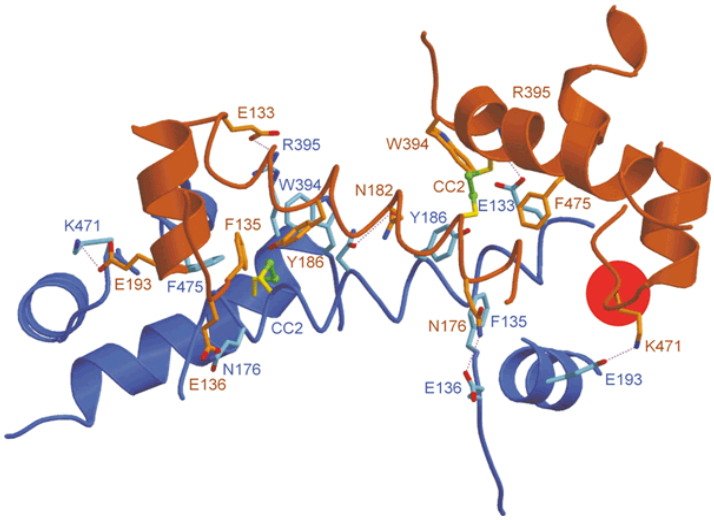

Figure 2. Ribbon model of the homodimer interface in *Brassica juncea* γ-glutamylcysteine ligase (BjGCL) highlighting the amino acids involved in the zipper-like contact zone (Gromes *et al.*, 2008)

The two monomers are depicted in blue and brown, respectively. Amino acid residues involved in the formation of the dimer interface and the core disulfide bridge are labelled with their position numbers. The site at which the second insertion is found in proteobacterial GCL proteins is marked with a red circle.

Redox regulation of GCL is also observed *in vivo*. Treatment of *Arabidopsis* seedlings

with 5 mM H_2O_2 induces a GCL shift from the less active reduced form to the more active oxidized form which leads to a two-fold increase in GCL activity (Hicks *et al.*, 2007). In addition, other stress treatments with cadmium, buthionine sulfoximine (BSO), or menadione (inducing ROS) alter GCL redox state similarly (Hicks *et al.*, 2007). However, oxidative stress induced by H_2O_2 does not increase transcription of the genes encoding GCL, although glutathione level are enhanced in these conditions (May and Leaver, 1993; Queval *et al.*, 2009; Willekens *et al.*, 1997; Xiang and Oliver, 1998). Thiol-based regulation of GCL offers a post-translational control mechanism for changing enzyme activity, thereby maintaining glutathione homeostasis in plants. Feedback inhibition of GCL by GSH is another regulatory mechanism (Hell and Bergmann, 1990; Jez *et al.*, 2004; Noctor *et al.*, 2002). To meet the demands for GSH consumption (e.g. detoxification of a range of xenobiotics) , this inhibitory effect on GCL is likely to be attenuated to facilitate the glutathione synthesis. Activity of enzymes can be influenced by the environment where they exist, especially in the case of redox-regulated GCL (Hicks *et al.*, 2007; Hothorn *et al.*, 2006; Jez *et al.*, 2004). GCL activity appears localized in the stroma of the chloroplast. Many metabolic enzymes in the stroma are active as reduced proteins and less active as oxidized, considering stroma as a reducing environment (Marty *et al.*, 2009; Rouhier *et al.*, 2008); however, the opposite situation occurs with GCL, for which the oxidized form is more active.

Arabidopsis GCL is encoded by a single gene. Knockout lines for AtGCL have a lethal phenotype at the embryo stage (Cairns *et al.*, 2006), Several GCL mutants have been previously identified by genetic approaches. The *rml1* mutant has about 3% of the wild-type amounts of GSH and it shows strong meristem defects (Vernoux *et al.*, 2000). In other GCL mutants with reduced glutathione contents, environment sensitivity is changed in spite of their weak growth phenotypes. The *cad2* mutant is susceptible to cadmium, and the *rax1* mutant constitutively expresses ascorbate peroxidase, whereas *pad2* has been identified by increased vulnerability to pathogen attack (Ball *et al.*, 2004; Cobbett *et al.*, 1998; Howden *et al.*, 1995; Parisy *et al.*, 2007).

1.1.3. Glutathione synthetase (GS)

In the second step of glutathione synthesis, Glutathione synthetase catalyzes the ATP-dependent formation of a peptide bond between the α-carboxyl group of cysteine in γ-glutamylcysteine and the α-amino group of glycine to form GSH. Structural characterization indicates that bacterial GS functions as a tetramer with four identical subunits of 35.6 kDa molecular weight each (Gushima *et al.*, 1984), whereas some mammalian, yeast, and plant GS are active as dimers (Gogos and Shapiro, 2002; Jez *et al.*, 2004; Polekhina *et al.*, 1999).

Several plant species produce analogs of glutathione such as homoglutathione and hydroxymethyl-glutathione (Klapheck *et al.*, 1994). The substrate glycine is replaced by β-alanine, serine, or glutamate in the glutathione variants. Homoglutathione is found in multiple legumes, using β-alanine instead of glycine (Moran *et al.*, 2000). Biosynthesis of glutathione and homoglutathione shares the synthesis of γ-glutamylcysteine, but the chemical variation depends on the specificity of the synthetases involved in the second reaction. It is reported that separate genes encode glutathione synthetase (GS) and homoglutathione synthetase (hGS) in *Medicago truncatula* , and hGS likely arose from GS by divergent evolution after the first duplication event (Frendo *et al.*, 2001).

GS transcripts prevalently encode a cytosolic protein and only a small fraction of GS protein is found in the plastids. It indicates γ-glutamylcysteine transport from plastids to the cytosol as location of GCL is exclusively confined to the plastids. In addition, proteome studies of *A. thaliana* suggest that neither GCL nor GS localized in mitochondria and peroxisomes, revealing the possibility of importing cytosolic GSH into the other GSH-containing compartments (Jimenez *et al.*, 1997; Jiménez *et al.*, 1998).

Knockouts of *GS* in *Arabidopsis* show a seedling-lethal phenotype during post-germination stage (Pasternak *et al.*, 2008). In *Arabidopsis*, hyperaccumulation of γ-EC cannot compensate the lack of GSH and prevent the lethal phenotype. However,

in bacteria and yeast accumulation of γ-EC can partially compensate the lack of GSH (Grant *et al.*, 1997). As γ-EC accumulation is not uncontrolled in GS mutants, a regulatory inhibition on GCL by γ-EC other than GSH is also likely. More investigation is needed for understanding detailed signaling mechanisms.

1.2. Glutathione degradation

The γ-glutamyl cycle, a pathway for the synthesis and degradation of glutathione, is of great importance for maintaining glutathione homoeostasis in plant. In this cycle, glutathione degradation is controlled by several enzymatic activities. Firstly, γ-glutamyl transpeptidase (GGT) cleaves the γ-glutamyl bond with broad substrate specificity, resulting in hydrolysis of GSH or its conjugated forms (Keillor *et al.*, 2005; Zhang *et al.*, 2005). The initial reaction yields the products γ-glutamyl amino acid and the Cys-Gly dipeptide. Dipeptidase hydrolyzes the Cys-Gly into the amino acid Cys and Gly which can be taken as substrates for GSH biosynthesis and used for extrusion (Ferretti *et al.*, 2009). The γ-glutamyl amino acid is converted to 5-oxoproline (5-OP) by γ-glutamyl cyclotransferase (GGCT) and then the 5-OP is cleaved into Glu by oxoprolinase (Ohkama-Ohtsu *et al.*, 2008). Another possible pathway for the initiation of GSH degradation involves carboxypeptidase or phytochelatin synthase (Beck *et al.*, 2003). In this pathway, the glycine moiety is cleaved off by breaking the C-terminus of glutathione, and the other moiety (γ-EC), may be then degraded to Cys and Glu. It is still very little known about this alternative metabolic route, although there is evidence showing GS-conjugates could be degraded by carboxypeptidase activity (Steinkamp and Rennenberg, 1985), which has been detected in barley vacuoles (Wolf *et al.*, 1996).

In plants, GGTs are located in extracytosolic (apoplastic and vacuolar) compartments. GGT isoforms have been purified from plant species including tomato, onion, and radish (Martin and Slovin, 2000; Shaw *et al.*, 2005). Functional analysis identified several GGT proteins in *Arabidopsis*, GGT1, GGT2, and GGT4 (Grzam *et al.*, 2007;

Ohkama-Ohtsu *et al.*, 2008; Ott *et al.*, 2007). GGT1, a cell-wall bounded protein, degrades oxidized GSH in the apoplast (Ferretti *et al.*, 2009) and GGT2 (also found in the apoplast) mediates GSH transport into siliques (Ohkama-Ohtsu *et al.*, 2007). GGT4 is located in the vacuole, where it is responsible for the degradation of GSH conjugates of toxic compounds and xenobiotics (Grzam *et al.*, 2007; Ohkama-Ohtsu *et al.*, 2008). Subcellular localization of GGCT and 5OPase seem to be in the soluble cytosolic fraction. The existing knowledge on GSH degradation in plants is still inadequate compared with that on GSH biosynthesis.

1.3. Glutathione compartmentalization and transport

Regulation of glutathione homeostasis by transport processes is crucial for maintenance of its biological function. As a long distance transport metabolite, glutathione provides reduced sulfur for shoot and root growth, as well as seeds development (Cairns *et al.*, 2006; Herschbach and Rennenberg, 2001). For example, mature Ricinus leaves synthesize and export GSH via the phloem. In addition, studies in spruce show GSH is exchanged between phloem and xylem (Schneider *et al.*, 1994). Independent evidence for inter-organ GSH transport also came from Adams and Liyanage (1993) who have shown that in grape, large amounts of GSH are imported from leaves to the fruits. Such extraction and uptake of GSH is mainly the result of extracellular conversion to other products. Recent studies have also demonstrated that several oligopeptide transporters (OPTs) in *Arabidopsis* encode components of the long-sought plasma membrane GSH transport machinery (Mendoza-Cózatl *et al.*, 2014; Zhang *et al.*, 2016).

In plant cells, GSH is mainly synthesized in chloroplasts and the cytosol, whereas the degradation of GSH and GS conjugates occurs in the vacuoles and perhaps in the apoplast. Such spatial separation of pathways may produce large GSH redox gradients between the various subcellular compartments. Therefore, glutathione transporters must be present in membranes such as vacuole and chloroplast for

maintaining the specific GSH-GSSG redox couples in each compartment (Foyer *et al.*, 2001; Jamai *et al.*, 1996; Noctor *et al.*, 2002; Pasternak *et al.*, 2008). However, the identity and the exact role of plasma membrane GSH-specific transporters still remains unclear, especially in plants (Bachhawat *et al.*, 2013).

Several different types of transporter may be crucial for glutathione exchange between subcellular compartments. Previous studies identified chloroplast envelope transporters that likely act to transport glutamylcysteine from plastids to cytosol (Maughan *et al.*, 2010). These transporters are decribed as CLT1, CLT2 and CLT3 in *Arabidopsis*. In addition, GSH can be imported from the cytosol into the chloroplast, as is shown by radio labelling studies in wheat (Noctor *et al.*, 2002). The transport of glutathione conjugates (GS-X) formed in the cytoplasm into the vacuoles in plants is facilitated by transporters of the ATP-binding cassette (ABC) family (Lu *et al.*, 1998). Investigation on the vacuolar transporters AtABCC1, AtABCC2, and SpAbc2 revealed that these transporters might play essential roles in vacuolar sequestration of phytochelatin/toxic heavy metals (Park *et al.*, 2012; Song *et al.*, 2010). Glutathione transport from the cytosol to the vacuole was also observed for oxidized glutathione (GSSG) under oxidative stress conditions (Queval *et al.*, 2011). A putative GSH transporter in rice may play a physiological role in retrieval of GSSG from the apoplast into the cytosol under stress conditions (Zhang *et al.*, 2004). ATP hydrolysis or co-transport mechanisms may drive glutathione transport through the membrane where energy input is required. Translocation of GSH into the nucleus could be facilitated by the incorporation or activation of GSH transport proteins such as Bcl-2 (Vivancos *et al.*, 2010b).

1.4. Function of glutathione

Multi-layer regulation on glutathione reveals its functional significance in plants (Noctor *et al.*, 2002). Exposing to environmental stresses triggers glutathione production, which acts as an anti-oxidant by quenching reactive oxygen species and

enters in the ascorbate-glutathione cycle that eliminates peroxides (Noctor and Foyer, 1998; Rouhier *et al.*, 2008). Glutathione is largely responsible for catalyzing conjugation reactions to detoxify xenobiotics (Labrou *et al.*, 2015) and protects against heavy metals by forming the metal-binding phytochelatins (PCs) (Yadav, 2010). It is also important for plant development and growth, cell proliferation and acclimation to various biotic and abiotic stresses (Mittova *et al.*, 2003; Parisy *et al.*, 2007; Vernoux *et al.*, 2000; Vivancos *et al.*, 2010a; Vivancos *et al.*, 2010b). The following chapter highlights some of these critical functions of glutathione.

1.4.1. Glutathione functions as an antioxidant and redox modulator

Reactive oxygen species (ROS) are natural by-products of the normal metabolism, e.g. photosynthesis and respiration (Sies *et al.*, 2017). Conversion of molecular oxygen (O_2) to water produces different types of ROS intermediates including hydroxyl radical ($OH\cdot$), superoxide anion radical ($O_2\cdot^-$), singlet oxygen ($^1O_2$) and hydrogen peroxide (H_2O_2). ROS are known to function in the control of redox homeostasis and cell signaling in which they act as signal mediators and second messengers under normal physiological conditions. However, unbalanced generation of these species leads to increased cell damage (eventually even cell death) by oxidation of macromolecules such as proteins and lipids (Møller, 2001). A tight control of the ROS network is critical for plants to cope with environmental fluctuations.

Glutathione is a major reservoir of non-protein reduced sulfur. Cellular glutathione remains in the millimolar range and this high amount is consistent with low glutathione redox potential values of plant cells (Meyer *et al.*, 2007). Therefore glutathione acts as a thiol buffer. Excess ROS can cause oxidation of the thiol group in GSH, resulting in accumulation of glutathione disulfide (GSSG) (Queval *et al.*, 2011). Perturbing the redox state of glutathione with stress has impact on different aspects of cell

metabolism.

GSH/GSSG, together with ascorbate/dehydroascorbate and NADPH/NADP, comprise three redox couples in the ascorbate-GSH cycle (Foyer and Noctor, 2011; Noctor and Foyer, 1998). This cycle reduces reactive oxygen species (ROS) in stress physiology, as it detoxifies hydrogen peroxide (H_2O_2) in plant cells (Asada, 1992; Noctor and Foyer, 1998; Shigeoka *et al.*, 2002). The primary peroxidation of ascorbate yields the monodehydroascorbate radical (MDHA) by ascorbate peroxidase (APX) which reduces H_2O_2 to water. MDHA is reduced back to ascorbate by monodehydroascorbate reductase (MDAR) or it is indirectly reduced through an intermediate dehydroascorbate (DHA) which is then converted to ascorbate by dehydroascorbate reductase (DHAR). Concomitantly, reduced glutathione (GSH) is oxidized to glutathione (GSSG). The oxidized glutathione dimers are recycled by a reaction catalyzed by GSH reductase (GR) using NAD(P)H as a reducing agent (Foyer and Halliwell, 1976; Noctor *et al.*, 2002; Noctor *et al.*, 2012).

Glutathione reductase (GR) is the key enzyme in GSH regeneration from GSSG. Although the GSSG can also be reduced by NADPH-thioredoxin reductase (NTR) (Marty *et al.*, 2009), however, GR is important for maintaining reduced glutathione in all subcellular compartments with exception of the organelles of the secretory pathway (Asada, 2006; Mullineaux and Rausch, 2005; Palma *et al.*, 2006; Reumann and Corpas, 2010; Wu *et al.*, 2013). A number of previous studies has also shown that overexpression of GR lead to an increase in cellular GSH levels in response to biotic and abiotic stresses (Foyer *et al.*, 1995; Kouřil *et al.*, 2003; Pilon-Smits *et al.*, 2000). Thus, a high activity of GR is necessary for plants to maintain high levels of GSH which is considered to be the most abundant soluble antioxidant (Signorelli *et al.*, 2013).

Although the ascorbate-glutathione cycle plays a major role in glutathione oxidation when H_2O_2 metabolism is increased, it is also noteworthy that specific enzyme systems (peroxidases) react rapidly with H_2O_2. Thiol peroxidases, including the glutathione peroxidases (GPXs) and the peroxiredoxins (PRXs), act as H_2O_2 and

organic peroxide scavengers. The reduction of the peroxide substrate occurs through thiol peroxidase cycle in which peroxiredoxins are subjected to post-translational modifications (PTMs). The regeneration of the thiol is facilitated by electron transmitters (e.g. TRX, NTRC, GRX) which receive electrons from redox input elements such as NADPH, ferredoxin (Fd), along with glutathione and ascorbate. Glutaredoxins (GRX) act as redox enzymes to catalyze the reduction of substrates by oxidation. Glutathione is a reducer of GRX. The oxidized glutathione is then renewed by GR. Taken together, these processes define glutathione system (Fernandes and Holmgren, 2004). The glutathione/glutaredoxin system is of great significance for maintaining cellular redox homeostasis (Grant, 2001).

1.4.2. Glutathione conjugates xenobiotics through glutathione S-transferases (GSTs)

Plants are continually exposed to toxic chemicals from environment. Such xenobiotics, including herbicides and chemicals used in industry, are nevertheless taken up and accumulate within the plant. Glutathione (GSH) plays an important role in the cellular detoxification machinery, preventing plant from hazardous xenobiotics. The well-characterized group of plant enzymes participating in xenobiotics detoxification are glutathione S-transferases (GSTs) (Riechers *et al.*, 2010). They catalyze a wide range of reactions involving the conjugation of glutathione to electrophilic substrates to form more soluble, less- or nontoxic peptide derivatives (Cummins *et al.*, 2013; Edwards and Dixon, 2005; Frova, 2003).

Over last decades, extensive studies have identified many glutathione transferases in various eukaryotes. Except for the Lambda and DHAR classes, which function as monomeric proteins (Lallement *et al.*, 2014), the soluble plant GST super-family form homo- and hetero-dimers. Each subunit of the dimer has a GSH binding site (G-site), mainly in the N-terminal domain, and a electrophilic substrate binding site (H-site) in the C-terminal domain (Marrs, 1996). Most classes of glutathione transferases have a

serine residue in their active site, yielding and stabilizing the reactive thiolate anion of GSH, whereas some other glutathione transferases possess a catalytic cysteine in their active sites which changes the enzyme catalytic properties. However, the catalytic Cys may act as nucleophilic agent on GSH-conjugates, which results in deglutathionylation and producing protein-glutathione adducts (Lallement *et al.*, 2014). Although GSTs are mostly cytosolic proteins, they have been found in the plastids, mitochondria, vacuole, nucleus and peroxisome (Dixon *et al.*, 2009a; Zybailov *et al.*, 2008). Conjugation of substrate to glutathione takes place in the cytosol and GSH-xenobiotic complexes are then sequestrated from cytosol into vacuoles by specific transporter. Once imported into vacuoles, GSH conjugates undergo further degradation processes (Grzam *et al.*, 2007).

GST-catalyzed glutathione conjugation detoxifies xenobiotics. Studies from different plant species have indicated the crucial role of this chemical modification scavenging toxic electrophiles. Overexpressing lines of the tau class GST isoenzyme GmGSTU4 from soybean exhibited significantly increased tolerance towards chloroacetanilide herbicide alachlor and showed reduced relative electrolyte leakage when treated with the diphenyl ether herbicides fluorodifen (Benekos *et al.*, 2010). *Arabidopsis* plants overexpressing two glutathione transferases (GSTs), GST-U24 and GST-U25 revealed strongly increased ability to withstand and detoxify the explosive 2,4,6-trinitrotoluene (TNT) (Gunning and Baron, 2014). In addition to catalyzing conjugation reactions, some glutathione transferases may have other functions, for instance, as peroxidase in antioxidative pathway (Dixon *et al.*, 2009b) or participating in biosynthetic pathways including the production of glucosinolates and camalexin (Dixon *et al.*, 2010).

1.4.3. Glutathione detoxifies heavy metals by phytochelatins (PCs)

Heavy metals are among most important factors that can cause damage to plants by

altering major plant physiological and metabolic activities (Rascio and Navari-Izzo, 2011; Villiers *et al.*, 2011). Common toxic metals are copper (Cu), iron (Fe), manganese (Mn) and zinc (Zn) (Duruibe *et al.*, 2007). Besides, some metalloids including antimony (Sb) and arsenic (As) are also toxic. Therefore a defense system in the plant is required for detoxification of these hazardous compounds. Phytochelatins (PCs) are metal binding cysteine-rich peptides, enzymatically synthesized in some fungi and plants from glutathione in response to heavy metal stress (Gadd, 2010).

Responses of plant cells towards heavy metals rely highly on glutathione (GSH) metabolism. On one hand, glutathione can detoxify heavy metals through control of ROS (as described above), as heavy metal poisoning induces ROS accumulation. On the other hand, glutathione governs the mobility of metals and metalloids through chelating peptides phytochelatins (PCs). PCs are rapidly generated after metal exposure and act as the main metal(loid) ligands which consist of repetitive γ-glutamylcysteine units within the $(\gamma\text{-Glu-Cys})_n\text{-Gly}$ (n=2-11) structure, and are synthesized from GSH by phytochelatin synthase (PCS) (Cobbett and Goldsbrough, 2002).

A large number of studies have revealed the contribution of GSH and PCs in heavy metal detoxification (Hirata *et al.*, 2005). PCs complex Cd and sequester it in vacuoles efficiently through the activity of ABC transporters. GCL mutants in *Arabidopsis* unable to synthesize PCs (*cad1-3*) were more sensitive to Cd and Hg than Col-0 (Sobrino-Plata *et al.*, 2014). *N. tabaccum* overexpressing glyoxalase pathway genes are tolerant to heavy metal stress by enhanced GSH and PCs levels (Singla-Pareek *et al.*, 2006). Other compartmentalization and translocalization can serve as additional strategies for heavy metal sequestration.

1.4.4. Glutathione in plant development and environmental responses

As the key regulatory component, Glutathione has gained increasing attention for its profound contribution to plant growth, development and defense against stressful environmental conditions, including pathogen attack (De Pinto *et al.*, 2012; Gadjev *et al.*, 2008). The importance of GSH in plant development has been revealed through the characterization of GSH-deficient *Arabidopsis* mutants. The GCL mutant *cad2-1,* which has a decreased capacity for GSH synthesis, produces fewer lateral roots and less root densities than the wild type (Schnaubelt *et al.*, 2015). Evidence from *Arabidopsis* triple mutant *cad2-1 ntra ntrb* indicated abnormal floral meristem development and decreased auxin transport (Bashandy *et al.*, 2010). Other implication comes from observation of a lethal phenotype in glutathione reductase knockout mutants which show impaired embryo development (Marty *et al.*, 2009).

Glutathione also appears to be involved in the cell cycle by providing an appropriate redox environment. GSH is localized in the nucleus during the cell cycle (Díaz-Vivancos *et al.*, 2010). Low GSH level is associated with decreased expression of genes that are necessary for cell cycle progression such as the G2 to M transition (Schnaubelt *et al.*, 2015).

The involvement of glutathione in plant response to biotic stress has been reported. *Arabidopsis* phytoalexin deficient 2-1 (*pad2-1*) mutant contains low level of GCL protein and exhibits glutathione deficiency. It shows high susceptibility to a wide range of pathogens (Parisy *et al.*, 2007; Schlaeppi *et al.*, 2008). Application of exogenous GSH can activate the expression of defense-related genes (Dron *et al.*, 1990; Wingate *et al.*, 1988). Regulation of the SA-dependent NPR1 (transcriptional co-activator) pathway is also associated with glutathione status (Després *et al.*, 2003; Mou *et al.*, 2003). All these findings reveal the important role the glutathione in

regulating plant defense.

1.5. Impact of redox homeostasis on proteins

Maintenance of cellular redox homeostasis is crucial for plants to adapt metabolic processes in changing environment. This redox homeostasis requires a well-balanced system in which ROS and antioxidant interaction is employed in a controlled manner. However, it is not yet fully understood how ROS is involved in regulation of signaling pathways. One mechanism to sense ROS is by modifying redox-reactive cysteine residues on proteins (Roos and Messens, 2011). This is well illustrated in activation of γ--glutamylcysteine ligase (GCL) through intramolecular disulfide bond formation (see previous chapter).

ROS-induced oxidation of redox-reactive cysteine residues include sulfenylation, sulfinylation, sulfonylation, and *S*-glutathionylation (Yu *et al.*, 2014). These oxidative modifications alter protein functions and redox signaling is thereby regulated for keeping redox homeostasis.

1.5.1. Oxidative modifications of proteins on cysteine residues

Post-translational modifications (e.g., phosphorylation, glutathionylation and ubiquitination) enable proteins having diversified functions by changing their properties such as conformation, catalytic capacity or stabilities. Cysteine (Cys) residues in proteins are major targets for post-translational modifications in ROS signaling. The thiol (-SH) group in Cys residues is subject to various redox-dependent modifications. Depending on logarithmic constant (pK_a) of a specific Cys, it reacts with ROS at different rates (Marinho *et al.*, 2014). Relative low pK_a renders the thiols act as a more reactive thiolate (RS-) and Cys is thereby prone to oxidation. Such oxidation can be reversible or irreversible. If oxidation by H_2O_2 is reversible, the protein thiol is defined as a “redox switch” (e.g., GCL) (Mailloux *et al.*, 2014).

Sulfenic acid (-SOH) is the initial oxidation state induced by minor ROS. As it is highly reactive and unstable, sulfenic acid may quickly react with neighboring thiol to form disulfide bonds or undergo further oxidation. The oxidation of sulfenic acid and disulfide are reversible and can be reduced by the thioredoxin (Trx) and the glutathione/glutaredoxin (GSH/Grx) systems with help of reducing equivalents (Bedhomme *et al.*, 2012; Schürmann and Buchanan, 2008).

Excessive ROS can further oxidize sulfenic acid to sulfinic ($-SO_2H$) or sulfonic ($-SO_3H$) acid. Sulfinylation and sulfonylation had long been considered as irreversible, however, the enzyme sulfiredoxin (Srx) was shown to reduce sulfinylated Prx (Biteau *et al.*, 2003). The highly oxidized sulfur species result in altered protein functions including enzyme inactivation and degradation.

Protein *S*-glutathionylation is an alternative modification forming a mix disulfide bond between a cysteine residue and gluthathione. It plays important role in redox signalling as well as protecting proteins from irreversible oxidation of protein thiols (Adachi *et al.*, 2004). *S*-glutathionylation is usually considered a modification occurring in response to enhanced production of ROS or oxidation of GSH to GSSG , although it also occurs under normal physiological conditions (Chen *et al.*, 2007). The modification can be reversible when the environment becomes more reducing. Glutaredoxin have been demonstrated to catalyze both glutathionylation and deglutathionylation on specific proteins (Dalle-Donne *et al.*, 2007). Proteomic approaches have identified many targets of glutathionylation associated with various processes such as protein folding and stability, signal transduction, intracellular trafficking, and apoptosis (Rouhier *et al.*, 2008). The specific functions of glutathionylation remain to be elucidated.

1.5.2. Redox regulation of MAPK-cascade

Mitogen-activated protein kinase (MAPK) cascades mediate signal transduction of diverse extracellular stimuli including pathogen attack, wounding, and abiotic stresses

as well as different physiological activities such as differentiation, proliferation and cell death (Romeis *et al.*, 2001).

MAPK cascades are a three-kinase module consisting of MAPK, MAPK kinases (MAPKK or MEK), and MAPKK kinase (MAPKKK or MEKK). MAPK is activated through dual phosphorylation of tyrosine and threonine residues in the TXY motif by MAPKK, which, in turn, is activated through phosphorylation of serine or threonine residues (Ser-X-X-X-Ser/Thr) within the catalytic center by a MAPKKK (Mizoguchi *et al.*, 1997; Zhang *et al.*, 1994). Many components of MAPK cascades were found in higher plants. However, the number of MEKs is far less than MAPKs, indicating protein cross-talk and redundancy in MAPK cascades.

Recent studies have revealed the correlation of MAPK cascades with ROS signaling. MKK3 can be activated by H_2O_2, and in addition, it mediates ROS production in response to wounding (Colcombet *et al.*, 2016; Takahashi *et al.*, 2011a). H_2O_2 activates a specific *Arabidopsis* MAPKKK (ANP1) and initiates the MAPK cascade, causing the phosphorylation of AtMAPK3 and AtMAPK6 (Lumbreras *et al.*, 2010). The over-expression of ANP1 orthologue NPK1 in tobacco plants, alleviates the effect of biotic or abiotic stresses (Kovtun *et al.*, 2000). Cadmium treated plant showed enhanced ROS level produced by oxidative stress as well as activated MAPK3 and MAPK6, which are regarded as positive regulators of defense responses (Liu *et al.*, 2010; Pitzschke *et al.*, 2009). Two tobacco orthologues of AtMAPK6 and AtMAPK3, salicylic acid induced protein kinase (SIPK) and wound-induced protein kinase (WIPK), respectively, seem to play an important role in environmental responses (Jonak *et al.*, 2002). SIPK was shown to be activated by ozone and H_2O_2 (Samuel *et al.*, 2000). Interestingly, transient activation of MAPKs in tobacco (WIPK and SIPK) and *Arabidopsis* (AtMAPK3, AtMAPK4 and AtMAPK6) is also related to increased glutathione biosynthesis, indicating possible impact of glutathione on MAPK signaling (Matern *et al.*, 2015).

In addition to MAPK activation by upstream kinase as mentioned above, MAPK can be deactivated by negative regulator phosphatases, including tyrosine-specific

phosphatases (PTPs), serine/threonine-specific phosphatases (PP2C) and also the dual-specificity phosphatases (DSPs) (Camps *et al.*, 2000; Keyse, 2000, 2008).

The dual-specificity MAPK phosphatases (MKPs) form a subgroup of DSPs and were shown to fully inactivate MAPKs by dephosphorylation of both, tyrosine and serine/threonine residues (Keyse, 2000). Five putative MKPs have been identified in A. thaliana (Bartels et al., 2010; Kerk et al., 2002). These MKPs vary in size and domain structure, but the active site is conserved. The critical cysteine residue (e.g., Cys109 in MKP2) in the consensus catalytic domain is necessary for phosphatase activity (Farooq and Zhou, 2004; Vilela *et al.*, 2010). Kamata *et al.* (2005) have reported ROS inactivation on mammalian MPK phosphatases via thiol oxidation of the cysteine residue in the active site.

Genetic and biochemical analyses have shown that AtMKP2 seems to be crucial in regulating oxidative stress-related responses. MKP2 can be induced by oxidative stress and its activation leads to dephosphorylation of AtMAPK3 and AtMAPK6 (Lee and Ellis, 2007; Lumbreras *et al.*, 2010). A hypersensitive ozone phenotype of MPK2-knockout line in *Arabidopsis* is related to ozone-triggered activation of AtMAPK3 and AtMAPK6 (Lee and Ellis, 2007). The subcellular co-localization into nucleus also indicates that MKP2 interacts with AtMAPK3 and AtMAPK6 in response to ROS (Lee and Ellis, 2007). *In vitro* evidence demonstrated that MAPK phosphatase 2 (MKP2) can be gluthathionylated (personal communication with Tatjana Peskan-Berghöfer and Sanja Matern). Under oxidative stress conditions, glutathionylation would inactivate the enzyme, but may prevent the MKP2 protein from degradation. On the other side, glutathionylation may also target the protein for degradation, as has been shown for human MPK1 (Kim *et al.*, 2012). However, there is still very little knowledge on MKPs post-translational regulation in plants, which remains to be clarified for better understanding of stress responses, whereby the thiol oxidation might be a possible way to control MKP2 function in plants.

2. Aims

Plants are facing various biotic or abiotic stresses. How plants cope with these external perturbations has been a critical issue, as unfavorable conditions could result in detrimental effects on plant growth and development, even leading to plant death. Understanding cellular regulatory mechanisms, especially regarding the stress responses needs close attention.

Recent studies have focused on glutathione modulation because of its multiple functions, not only related to stress responses, but also for maintenance of cellular redox homeostasis during plant development. Therefore, controlling glutathione level by its biosynthesis is of great importance. Given that glutamate cysteine ligase (GCL) catalyzes the rate-limiting step of GSH synthesis, this enzyme seems to play a pivotal role in this control. However, the existing knowledge is still not sufficient to elucidate the molecular mechanism of GCL regulation. This work aims at characterizing GCL activation at the mechanistic side, in particular, exploring the possible link between the formation of the regulatory intramolecular disulfide bridge in plant GCL (Hicks *et al.*, 2007; Hothorn *et al.*, 2006) and the simultaneous formation of homodimers (Gromes *et al.*, 2008). We mainly focus on evaluating the contribution of dimer formation to GCL activity using biochemical approaches.

It has been indicated that the MAPK cascade is involved in oxidative stress signaling. As MKP2 modulates the activities of MAPKs, it is predicted that MKP2 may be regulated by oxidative stress. The active site cysteine (Cys109 in MPK2) is necessary for phosphatase activity and conserved among all MKPs from the plant and animal origin. In mammals, this conserved Cys residue is redox-sensitive, and responsible for protein degradation upon oxidation. Up to date, the post-translational modulation of MKP2 remains largely unknown in plants. Thus another focus of this work is to explore redox-dependent control of MKP2.

3. Results

3.1. Generation of recombinant AtGCL proteins mutagenized at the dimer interface

3.1.1. Mutagenesis of recombinant AtGCL variants

According to the knowledge on GCL regulation, it is still unclear whether formation of an intramolecular disulfide bond is sufficient for GCL enzyme activation, or if the subsequent homodimerization is also a necessary step for activation. To answer this question, amino acid residues forming the dimer interface were mutated in order to disrupt the dimerization state and biochemically characterize the recombinant GCL activities. Previous study has shown that amino acid residues contributing to the zipper-like dimer interface are conserved among all higher plant GCL sequences, highlighting several salt bridges as well as hydrophobic side chains (Gromes *et al.*, 2008). Therefore, after comparing protein sequences between AtGCL and BjGCL (Figure S 1), we decided to mutagenize AtGCL at the following mutation sites shown in Table 1. Either one or two amino acid residue(s) within GCL sequence were changed for each GCL variant. Site-directed mutagenesis was used to clone the ORFs coding for GCL. The corresponding wild-type and mutated proteins were overexpressed in *E. coli* .

Table 1. Overview on GCL mutations in *Arabidopsis thaliana*

The mutated amino acid residues are highlighted in red. The asterisk (*) indicates soluble mutant proteins.

	AtGCL amino acid pairs	Mutated AtGCL amino acid pairs
Redox	Cys186/Cys406	Ser186/Cys406 * Cys186/Ser406 * Ser186/Ser406
Salt bridges	Glu141/Arg403	Lys141/Arg403 Glu141/Glu403 * Gln141/Met403 *
	Glu201/Lys479	Lys201/Lys479 * Glu201/Glu479 * Gln201/Met479
		Lys141/Arg403 and Glu201/Glu479 *
Hydrophobic interactions	Phe143/Trp402	Leu143/Trp402
	Tyr194/Phe483	Leu194/Phe483 *
		Leu143/Trp402 and Leu194/Phe483

3.1.2. Expression of recombinant AtGCL variants in *E.coli*

As shown in Figure 3, wild-type *Arabidopsis* GCL was purified by nickel affinity chromatography. The protein was induced by IPTG and unspecific proteins were washed off by standard washing buffer containing 200mM imidazole (Figure 3A). Because the GCL protein was partially washed off the column due to a high concentration of imidazole, a series of washing buffers containing imidazole in different concentrations were tested for optimizing the washing condition (Figure 3B). The result showed that 45mM imidazole was suitable for washing off unspecific

proteins and keeping GCL attached to the column. After purification for two times (before and after TEV cleavage), the wild-type GCL was collected and detected as a protein band having a size of about 51kD by western blot analysis (Figure 3D).

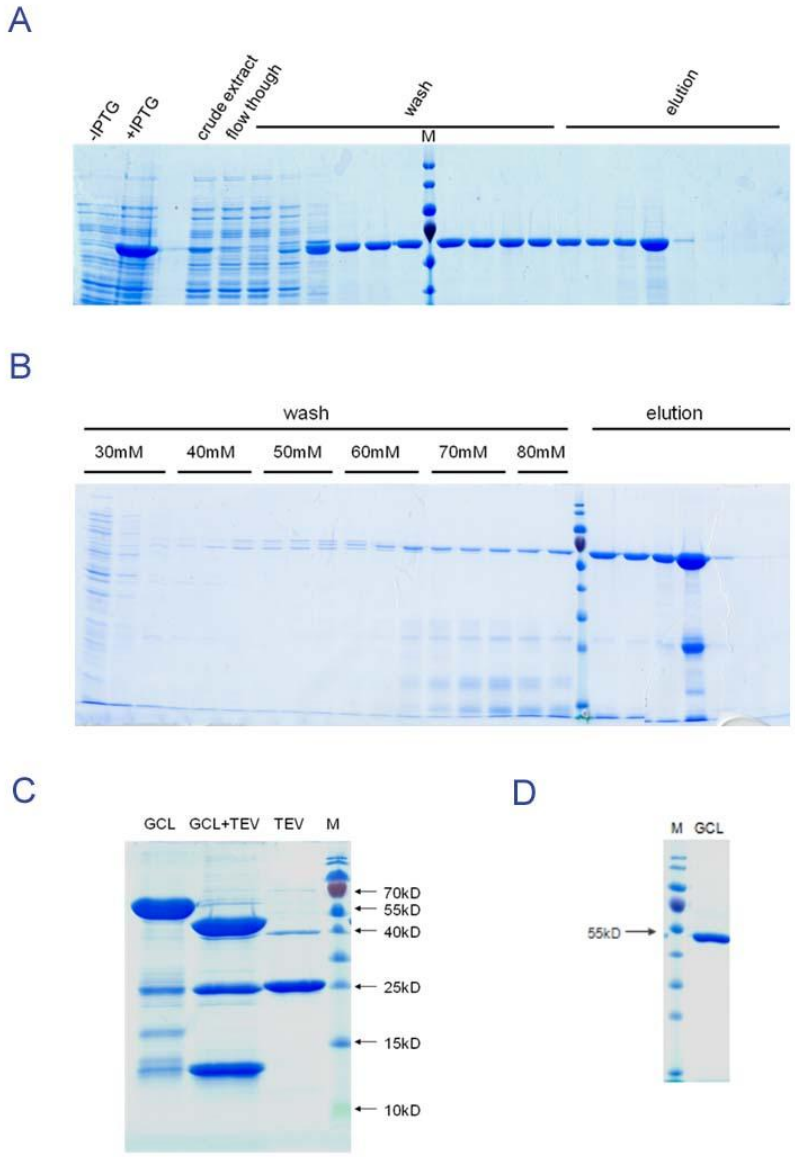

Figure 3. Purification of wild-type GCL shown by SDS-PAGE.

A. 1st affinity chromatography. Protein (fused with His tag and thioredoxin) was bound to a Ni^{2+}-NTA column and eluted (about 64kD) after the washing step with 200mM imidazole.

B. Optimization of imidazole concentrations during 1st affinity chromatography. A series of imidazole concentrations ranging from 30mM to 80mM were tested for washing off unspecific proteins.

C. Comparison of un-cleaved and cleaved wild-type GCL. The first lane shows the

purified fusion protein after 1st affinity chromatography. The second lane shows the result of dialysis of the protein with TEV protease. The mixture contained cleaved wild-type GCL together with TEV (about 25kD), His and thioredoxin (below 15kD).
D. Finally purified wild-type GCL (about 51kD) After separation of cleaved GCL from TEV, His and thioredoxin by binding to a second Ni^{2+}-NTA column. The GCL was eluted as a protein of about 51kD and concentrated by centrifugal filtration. Protein samples were run under denatured conditions.

Similar to the wild-type GCL, other mutated GCL variants listed in Table 1 were purified by nickel affinity chromatography as well. Figure 4 demonstrates three examples of purified GCL mutants. In the mutant protein Ser186/Cys406, one disulfide bond was abolished because of the replacement of Cys186 with Ser186. As shown in Western blot result (Figure 4A), this mutant was soluble after purification. Similar results were observed when we purified the mutant Cys186/Ser406, whereas the mutant Ser186/Ser406 could not be purified. Figure 4B illustrates another mutant, Lys141/Arg403 and Glu201/Glu479, in which Glu141 is replaced by Lys141, and Lys479 is replaced by Glu479 respectively. Indeed, we could still purify the mutant protein even though two salt bridges involving zipper-like contact zone were disrupted in this case. Regarding the mutant Leu143/Trp402 and Leu194/Phe483, although the protein induction by IPTG in *E. coli* was successful, the protein was missing in the elution fraction after first purification step (Figure 4C). In this mutant, hydrophobic side chains were disrupted due to the replacement of Phe143 to Leu143 and Tyr194 to Leu194 respectively. In addition to these three mutants, other protein variants listed in the table 1 were subjected to purification as well. Some mutants were soluble whereas some were not after purification. The reason may be the misfolding or unfolding of the mutants which results in protein aggregation.

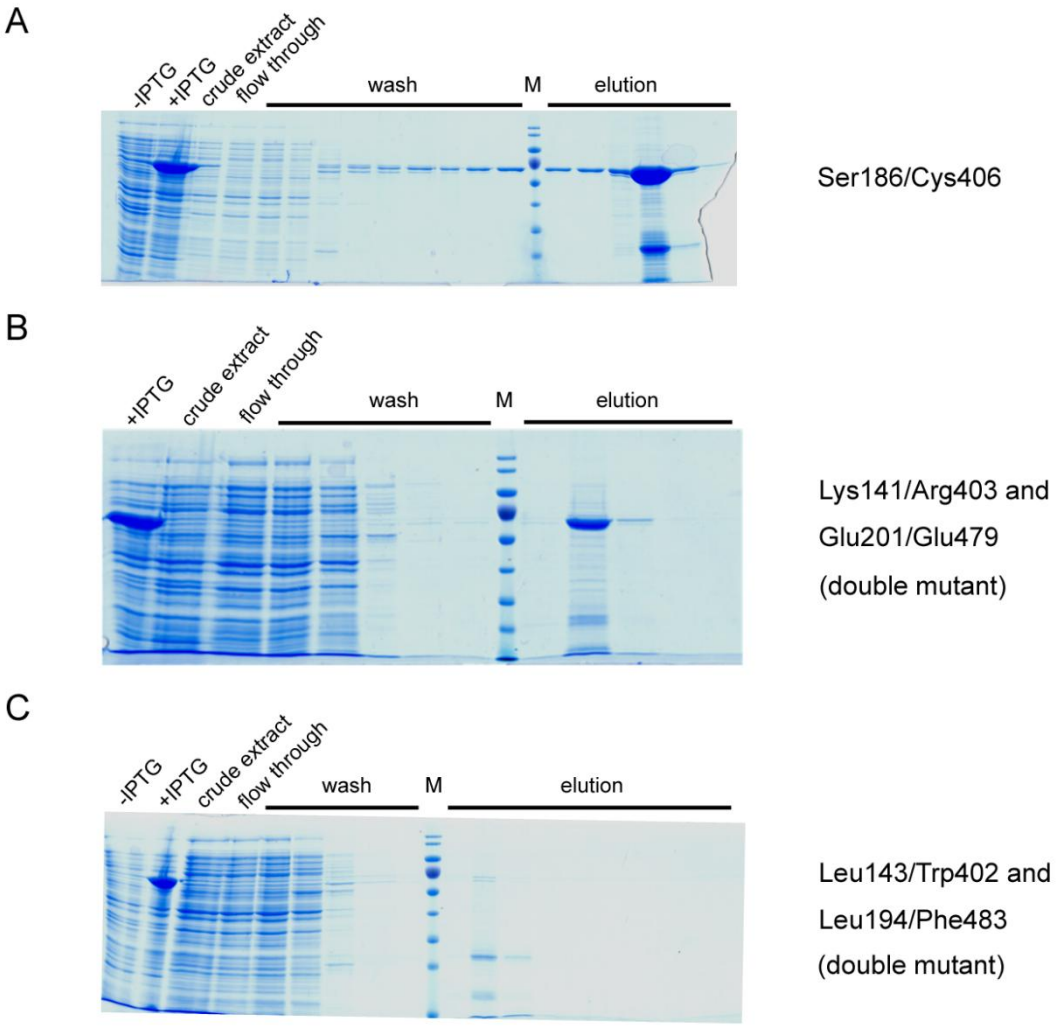

Figure 4. Purification of recombinant GCL variants.

1st affinity chromatography results for recombinant GCL mutants were shown by SDS-PAGE. Proteins (fused with His tag and thioredoxin) were induced by IPTG in *E. coli*. Proteins were bound to a Ni^{2+}-NTA column and eluted (about 64kD) after washing steps with imidazole. Protein samples were run under denatured conditions. Purification of recombinant GCL variant Cys186/Ser406, Lys141/Arg403 and Glu201/Glu479, Leu143/Trp402 and Leu194/Phe483 was shown in A, B and C, respectively.

3.2. Dimer formation is disrupted in GCL mutants

The results described in this section are adapted from the submitted manuscript Yang *et al.*, 2018.

3.2.1. Redox-state profiles of mutated GCL proteins

To examine the mobility profiles of recombinant AtGCL WT and mutated variants, only four representative mutants were shown in the following studies (Figure 5). Upon analysis under reduced conditions, it has been observed that all the recombinant proteins, including WT and mutants, behaved similarly. Each of them ran as one reduced band with molecular mass of approximately 50 kDa, as we expected. However, under non-reducing conditions, the profiles of recombinant protein were varying. The mutants Glu141/Glu403 and Lys201/Lys479 showed similar patterns, comparable to that of WT GCL. They were present predominantly as oxidized forms, while a small portion appeared as a reduced form. For mutants Gln141/Met403 and Leu194/Phe483, the relative ratio of oxidized to reduced form was not as high as that for WT GCL. Noteworthy, we could only observe the oxidation states of the GCLs other than oligomeric forms due to 0.1% w/v SDS in the running buffer in non-reducing SDS-PAGE.

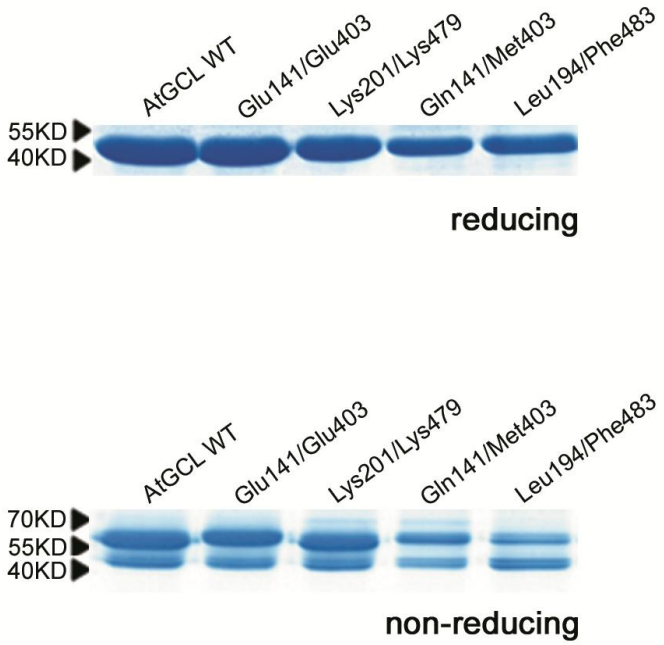

Figure 5. Analysis of WT and mutant AtGCL proteins via reducing and non-reducing SDS-PAGE

After recombinant expression in *E. coli* (see Materials and Methods), proteins were separated by SDS-PAGE. Under reducing conditions (+ β-mercaptoethanol), all GCL proteins were detected via Coomassie blue staining as single bands of the predicted size (~ 50 kDa), whereas under non-reducing conditions (- β-mercaptoethanol) all GCL proteins displayed oxidized (upper band) and reduced (lower band) form. Proteins were stained with Coomassie blue. Arrowheads correspond to Mr markers.

3.2.2. Size-exclusion chromatography confirms that dimer formation was disrupted in mutated GCL proteins

Size-exclusion chromatography (SEC) was performed to investigate oligomeric states of GCL variants. As shown by the previous data (Gromes *et al.*, 2008). WT AtGCL behaved predominantly as a dimer at a volume corresponding to 106 kDa under non-reducing conditions (Figure 6). Under reducing conditions (DTT treatment), the protein eluted as the 50 kDa species, where the monomer should be eluted. When the mutants were applied, we only observed elution peak at a volume corresponding to the monomer size, irrespective of pre-treatment with reducing agent. It indicated that the mutant proteins could not form dimer and that mutation in only one of the contact sites, previously determined by protein structure analysis (Hothorn *et al.*, 2006), was sufficient to disrupt dimer formation.

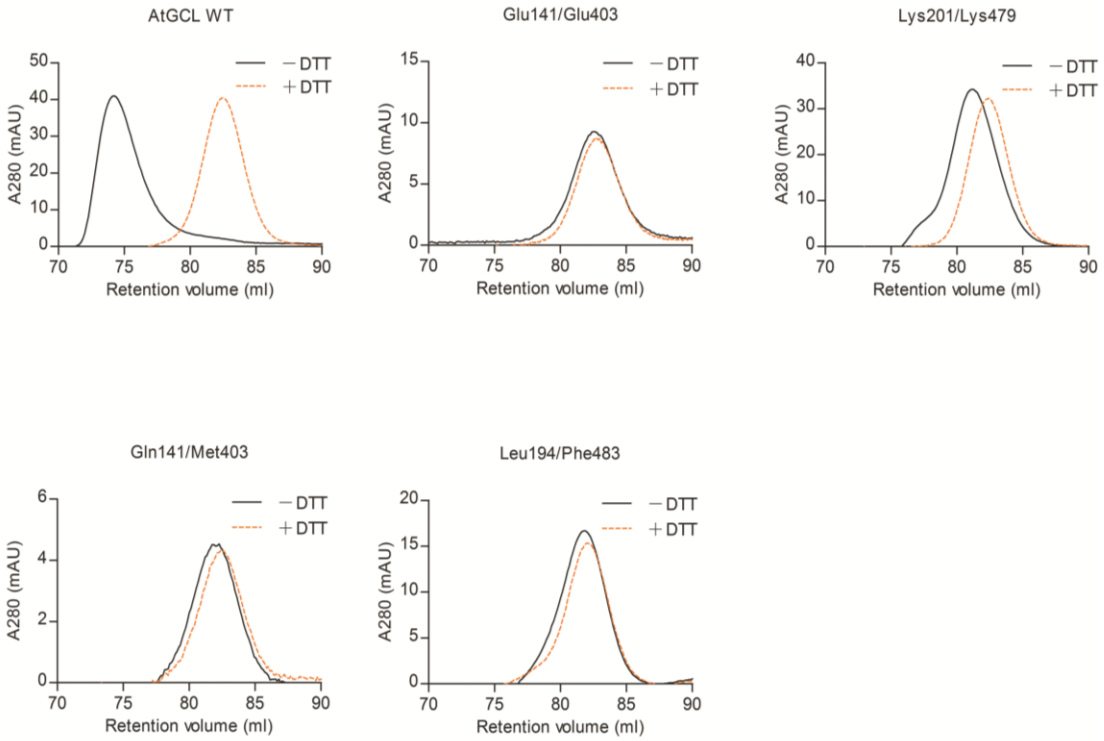

Figure 6. Size-exclusion chromatography of WT and mutant AtGCL proteins in the absence or presence of DTT

After dialysis overnight at 4 °C in buffer (25 mM HEPES (pH 7.5), 150 mM NaCl, and 5 mM $MgCl_2$), purified proteins were loaded onto a Superdex-200 FPLC column. WT AtGCL protein eluted predominantly as dimer under non-reducing conditions (black) and as monomer under reducing conditions (orange) (in the presence of 120 mM DTT). According to the retention volume, the estimated Mr values of AtGCL dimer and monomer corresponded to 106 kDa and 50 kDa, respectively, the predicted Mr for AtGCL monomer being 50.9 kDa. All mutant GCL proteins eluted predominantly as monomer under reducing and oxidizing conditions.

3.2.3. Ionic strength affects dimer-monomer transition of WT GCL

There is some evidence showing that the ionic strength in the protein buffer could impact protein-protein interactions (Aymard *et al.*, 1996). This influence was also evaluated in GCL proteins by SEC. Different NaCl concentrations were used in the elution buffer. Under low ionic strength (10 mM NaCl) (Figure 7A) without DTT

treatment, the active and dimerized (i.e. oxidized) WT AtGCL protein eluted similarly as in the presence of 150 mM NaCl (shown in Figure 6). Nevertheless, after DTT treatment the elution profile of WT GCL differed between 10 mM and 150 mM NaCl. Both dimer and monomer were observed at low ionic strength, whereas at high ionic strength only monomer form was observed. Furthermore, we examined the elution profile for one of mutant proteins, Gln141/Met403, in which a salt bridge in the dimerization interface was disrupted (Figure 7B). The result showed that there was no difference between the elution patterns if either 150 mM or 10 mM NaCl was applied in the buffer. By disrupting the dimer interface in this mutant, the protein eluted as monomer with or without DTT treatment in the presence of 10 mM NaCl. It behaved in the same manner when using 150 mM NaCl in the elution buffer (Figure 4).

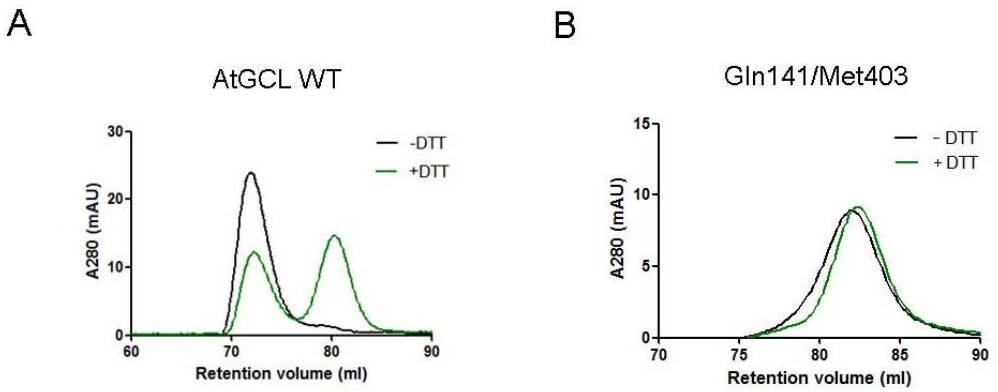

Figure 7. Size exclusion chromatography (SEC) of AtGCL proteins at low ionic strength

A. SEC analysis of WT AtGCL protein in the presence of 10 mM NaCl (instead of 150 mM NaCl; see Figure 6). While without DTT pre-treatment the oxidized protein eluted as a dimer (black), the pre-treatment with DTT did not induce complete conversion to monomeric state (green), indicative of ionic interactions at the dimer interface that were not completely disrupted by 10 mM NaCl.
B. SEC analysis of mutated protein Gln141/Met403 in the presence of 10 mM NaCl (instead of 150 mM NaCl; see Figure 6).

3.2.4. Certain range of pH variation does not affect dimer-monomer transition of recombinant GCL

pH is another decisive factor which may have an influence on dimer-to-monomer transition (Mohan *et al.*, 2006). Considering the GCL protein localization in the stroma of chloroplast, the physiological variation of pH value is between pH 7 (dark phase) and pH 8 (light phase). Based on that, pH 7 and pH 8 was used for comparing the effect. The results demonstrated that the elution behavior of WT AtGCL protein did not reveal a significant change in elution profile (Figure 8A), indicating that the GCL dimer is stable within this pH range.

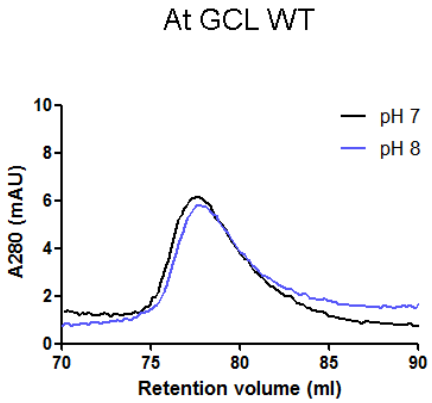

Figure 8. Size exclusion chromatography (SEC) of AtGCL proteins under different pH conditions

SEC analysis of WT AtGCL protein at pH 7 and pH 8 (instead of pH 7.5 used in Figure 6). WT AtGCL protein eluted similarly as dimer under both conditions.

3.3. GCL dimer formation does not contribute to redox-mediated enzyme activation

The results described in this section are adapted from the submitted manuscript Yang *et al.*, 2018.

3.3.1. Disruption of dimer formation in mutated GCL proteins does not render significant reduction of WT enzyme activities

After we confirmed that the mutated GCL proteins did not form dimer anymore, the enzyme activity assay was carried out for evaluating the contribution of dimerization to GCL activation. A standard assay coupling two additional enzymatic reactions was performed and the results are shown below (Figure 9). In accordance with previous reported data, the specific activity of oxidized WT GCL was 112.3 nmol min^{-1} mg^{-1} whereas after DTT treatment, its specific activity decreased to less than 50 nmol min^{-1} mg^{-1}.The mutants Glu141/Glu403 and Lys201/Lys479, which remained as the predominantly oxidized monomers, showed 86 % and 77 %, respectively, of WT AtGCL activity. In contrast, the less-oxidized mutants Glu141/Met403 and Leu194/Phe483 had specific activities significantly different from that of WT GCL without DTT treatment. The strongest reduction of specific activity was displayed in the mutant Ser186/Cys406 disrupting the regulatory disulfide bond. The DTT effects in Glu141/Glu403 and Lys201/Lys479 were similar to that in WT GCL while in the mutants Glu141/Met403, Leu194/Phe483 as well as Ser186/Cys406, reduction by DTT did not impact on specific activities so much as that in WT GCL. Taken together, it implied that disruption of dimerization had little influence on enzyme activity and the oxidation played the major role for GCL activation.

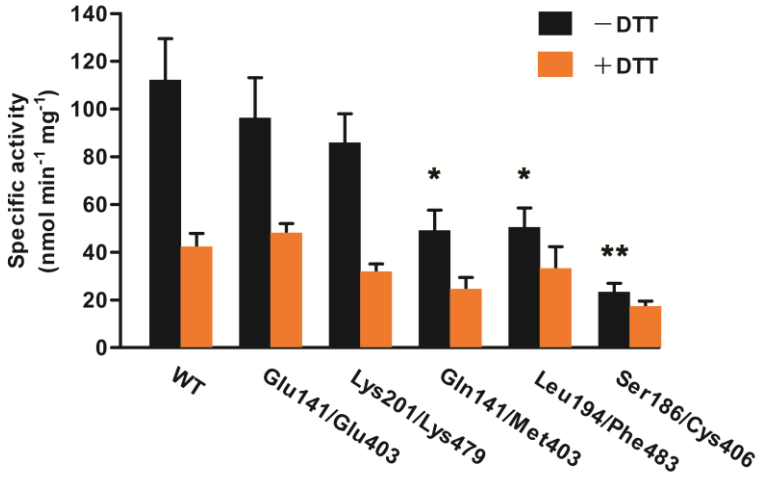

Figure 9. Specific enzyme activities (Vmax) of WT and mutant AtGCL proteins in the absence or presence of DTT

Values for specific activities (nmol min^{-1} mg^{-1}) are expressed as means ± S.E; (n>3). Significant differences of GCL mutants (without DTT) as compared to the WT (without DTT) are indicated by asterisk (*) (Student's T-test, *P ⩽ 0.05, **P ⩽ 0.01).

3.3.2. Disruption of the dimer formation does not affect the affinity of GCLs for their substrates

To examine the impact of dimerization of GCL on substrate affinity, K_m values of GCL variants including WT and mutants were determined for three substrates: glutamate, ATP and cysteine (Table 2). The results showed that K_m values for the substrates were in the same range for the WT GCL and the mutants. It indicated that the introduced mutations disrupting dimerization did not significantly interfere with the active site.

Table 2. Km values of WT and mutant AtGCL enzymes for cysteine, ATP and glutamate

Enzyme assays were performed as described under Materials and Methods. Values for specific activities (nmol min^{-1} mg^{-1}) are expressed as a mean ± S.E. (n=3).

	K_m Values		
	Cysteine	Glutamate	ATP
AtGCL WT	0.35 ± 0.06	6.64 ± 0.5	1.25 ± 0.08
Glu141/Glu403	0.33 ± 0.12	7.56 ± 0.26	1.16 ± 0.02
Lys201/Lys479	0.12 ± 0.02	8.42 ± 0.44	1.45 ± 0.14
Gln141/Met403	0.44 ± 0.14	6.99 ± 0.41	1.43 ± 0.10
Leu194/Phe483	0.08 ± 0.02	9.25 ± 0.50	1.50 ± 0.06

3.4. Probing the dimerization state of AtGCL protein extracted from plant leaf discs

The results described in this section are adapted from the submitted manuscript Yang *et al.*, 2018.

In order to clarify the dimerization state of endogenous AtGCL protein, we firstly conducted the oxidative stress treatment by using leaf discs from *Arabidopsis* seedlings (Hicks *et al.*, 2007) (Figure 10B). The treatment with H_2O_2 caused GCL to appear as a more oxidized form. A total plant extract from the leaf discs was applied onto FPLC column for protein separation. Eight consecutive fractions collected after elution were subjected to SDS-PAGE and immunoblot to detect the GCL protein. As shown in Figure 10A and B, GCL was eluted in the fraction 5 where it corresponded to the GCL monomer, despite being predominantly in the oxidized state. To assess whether the predominantly monomeric state of oxidized endogenous AtGCL was the result of its low concentration in the plant extract, the effects of different concentrations of recombinant WT AtGCL protein was examined by FPLC analysis (Figure 10C-E). It revealed that by decreasing the protein amount loaded to FPLC column, the profile shifting from dimer to monomer occurred. In addition to that, the different fractions collected were also subjected to immunoblot analysis by using GCL specific antibody to further determine the oxidation state of the GCL protein (Figure 10F-H). When the amount of oxidized recombinant AtGCL in the loaded sample was reduced from 50 µg to 7.8 or 2.2 µg, respectively (corresponding to a concentration of 10^{-6} M, 1.5 x 10^{-7} M and 4.4 x 10^{-8} M, respectively) the elution profile changed from a predominantly dimeric state (Figure 10F) to the monomeric state (Figure 10H). The proteins under three different concentrations all behaved as the oxidized forms. The signal intensities of fraction 3, 4 in Figure 10F and of fraction 4, 5 in Figure 10G seemed to be very similar, this may result from the over-exposure time during the detection in Western blot analysis.

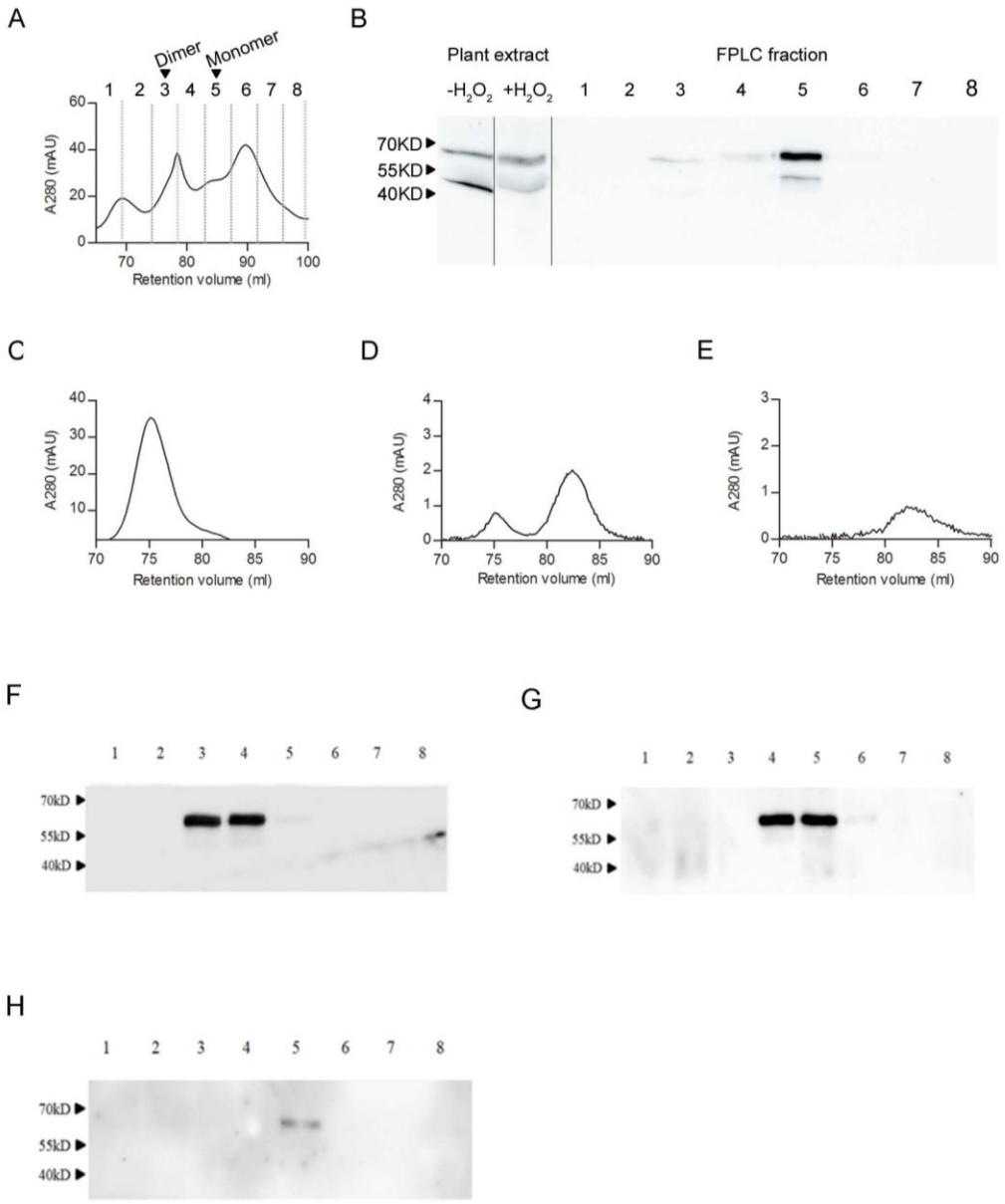

Figure 10. FPLC elution profile of endogenous AtGCL in total protein extract from H_2O_2-treated leaf discs as compared with elution profiles for different amounts of recombinant WT AtGCL protein

A. protein elution profile (280 nm) of *Arabidopsis* total protein extract from leaf discs pre-treated with 5 mM H_2O_2 for one hour; total protein was extracted from rosette leaves of 4-week-old WT *Arabidopsis* plants.

B. comparison of ratio oxidized/reduced AtGCL in extracts of control versus H_2O_2-treated leaf discs (left panel) and immunoblot analysis of eluted fractions after FPLC of extract from H_2O_2-treated leaf discs after SDS-PAGE under non-reducing conditions (right panel, for fraction number see A); the predominantly oxidized endogenous AtGCL protein elutes as monomer (fraction 5).

C-E. FPLC elution profiles for different amounts of recombinant WT AtGCL protein (1

nmol [C], 0.15 nmol [D], 0.044 nmol [E]; corresponding to concentrations of 10^{-6} M, 1.5 x 10^{-7} M and 4.4 x 10^{-8} M, respectively).
F-H. Immunoblot analysis of elution fractions from different amounts of recombinant WT AtGCL protein (F: 50 µg; G: 7.8 µg; H: 2.2 µg) after SDS-PAGE under non-reducing conditions. Molecular weight markers are indicated by arrows.

3.5. Quantification of endogenous GCL protein in *Arabidopsis thaliana*

The results described in this section are adapted from the submitted manuscript Yang *et al.*, 2018.

In order to determine the AtGCL concentration *in vivo*, we did the dot blot analysis, comparing the proteins from leaf extraction with recombinant AtGCL. The result is shown in the following figure (Figure 11). From a dilution series of both plant extract and recombinant protein, we could find comparable protein amounts and deduced the endogenous AtGCL concentration in the chloroplast would be in the millimolar range.

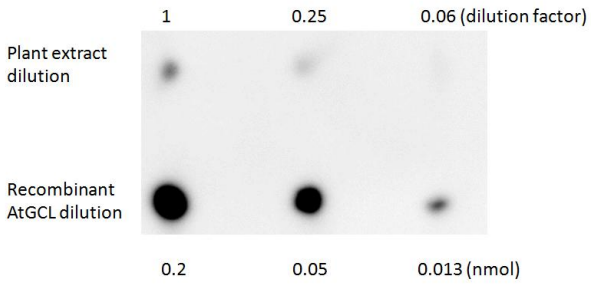

Figure 11. Quantification of AtGCL protein in *Arabidopsis* leaf extract by comparative dot blot analysis of leaf protein extract with dilution series of recombinant AtGCL protein

Dot blot analysis of recombinant AtGCL protein (0.2, 0.05 and 0.013 nmol) compared with different leaf protein extract dilutions. Undiluted extract (1) corresponded to 2.2 µg protein (equivalent to 0.4 mg fresh weight). The comparison indicates that the amount of endogenous AtGCL protein in 0.4 mg of leaf tissue approximately equals 0.013 nmol of recombinant AtGCL protein, corresponding to 32 nmol endogenous AtGCL protein per kg fresh weight.

Besides using leaf extracts as material to estimate endogenous GCL protein concentration in plastids, a dilution series of *Arabidopsis* root extracts and recombinant AtGCL proteins were compared to each other to analyze GCL amount (Figure 12); total proteins were extracted from the root part of *Arabidopsis* instead of leaves to minimize distortion of GCL immune signals. The specific GCL protein bands detected by western blot (other than dot blot) were compared with each other to make a more direct result. The endogenous AtGCL concentration was approximately estimated to be 0.5×10^{-3} M. Considering a total plastidial volume in roots corresponding to less than 10% of total tissue volume, as an conservative estimation, the AtGCL concentration in plastids is proposed to be at least 5×10^{-3} M. This value is in the concentration range where oxidized GCL protein is expected to form dimers.

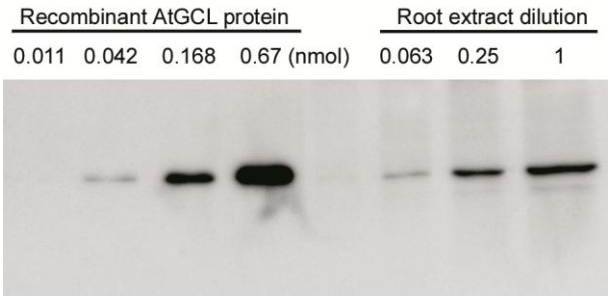

Figure 12. Quantification of AtGCL protein in *Arabidopsis* root extract by immunoblot analysis of root protein extract with a dilution series of recombinant AtGCL protein

Recombinant AtGCL protein (0.011, 0.042, 0.168 and 0.67 nmol) as compared with different root protein dilutions. Diluted extract (0.063) corresponded to 0.3 µg protein (equivalent to 0.078 mg fresh weight). The comparison indicates that the amount of endogenous AtGCL protein in 0.078 mg of root tissue approximately equals 0.042 nmol of recombinant AtGCL protein, corresponding to 538 µmol endogenous AtGCL protein per kilogram fresh weight.

In addition, we tried to examine the equilibrium of GCL dimer and monomer using the approach of Isothermal titration calorimetry (ITC). The result was shown in Figure 13. The binding affinity of protein was analyzed by ITC at pH 7.5 and it turned out that when the applied protein concentration is very low, the signal can not be detected (data not shown). However, by titrating higher concentration of GCL (450 µM), we could obtain an equilibrium dissociation constant of 90 µM (Figure 13). This Kd is likely to represent the equilibrium between dimer and oligomer since under concentration of 450 µM, GCL is presumably in the state of dimer. Change in enthalpy (ΔH) and change in entropy (ΔS) were calculated in the assay as -1.86 and -0.16, respectively.

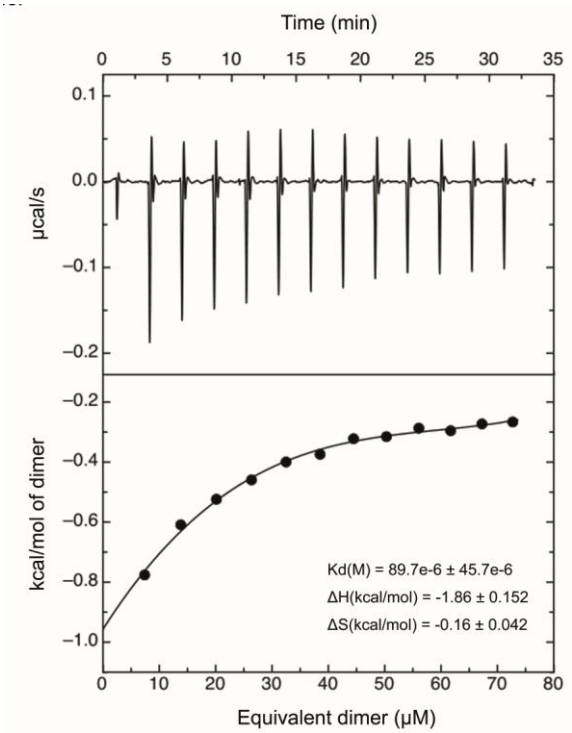

Figure 13. Isothermal titration calorimetry analysis of recombinant AtGCL dissociation

Protein samples were dialyzed overnight in ITC buffer. For determination of the dissociation constant (Kd) of *A. thaliana* GCL the syringe was loaded with GCL (450 µM) and titrated into the sample cell filled with ITC buffer. ITC data were processed using the MicroCal PEAQ-ITC Analysis Software and thermodynamic parameters were obtained by fitting the data to a dissociation model (for further details see Materials and Methods). The experiments were performed in triplicate. Kd, dissociation constant; ΔH, change in enthalpy; ΔS, change in entropy.

3.6. Redox-dependent control of GCL during the stress treatment

3.6.1. Redox sensitivity of GCL upon H_2O_2 treatment

It has been reported that plant GCLs respond to oxidative stress both *in vivo* and *in vitro* (Hicks *et al.*, 2007; Hothorn *et al.*, 2006; Jez *et al.*, 2004). To further understand how the redox state of GCLs is altered for perceiving the changes in the redox

enviroment, *Arabidopsis* seedlings were grown on MS medium and then subjected to water or hydrogen peroxide treatment. Only the root tissue of *Arabidopsis* was used for protein extraction in order to reduce the interference of Rubisco which has similar mobility in the gel as GCL. As shown in Figure 14A, a similar pattern was observed for both, 5 mM or 10 mM hydrogen peroxide treatment. By increasing the treatment time of H_2O_2 up to 5 hours, a redox state shift (more oxidized and less reduced GCL) was observed, whereas after 24 hours of incubation with H_2O_2, the ratio of oxidized to reduced form has decreased again. This may result from the long-time treatment disturbing cellular homoestasis. Remarkably, the signals of oxidized form were stronger, especially in samples treated with 2 h or 5 h H_2O_2 than those of controls treated with water, suggesting that GCL does respond to oxidative stress (hydrogen peroxide). This is in accordence with previously reported data. We always observed multiple bands of reduced GCL from *Arabidopsis* root extract, the reason may attribute to the disulfate bonds or modification on protein itself which remains to be further explained by biochemistry approaches.

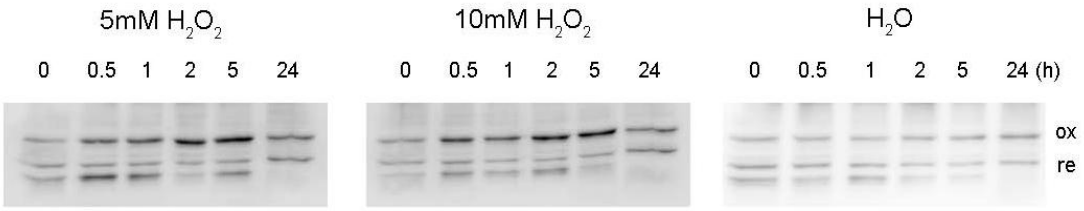

Figure 14. Redox sensitivity of GCL by hydrogen peroxide treatment

Arabidopsis seedlings were grown on ½ MS medium for two weeks and treated with H_2O_2 (5mM, 10mM) or H_2O for 0-24 hour. Protein extracts from root tissue of seedlings were subjected to SDS-PAGE under non-reducing conditions followed by immunoblot analysis using antisera against AtGCL. The oxidized and reduced GCL were labelled with ox and re, respectively. The reduced GCL was always detected as multiple bands.

3.6.2. Redox sensitivity of GCL upon cycloheximide (CHX) treatment

Cycloheximide (CHX) is a cell-permeable molecule that specifically inhibits protein synthesis in eukaryotic organisms (Chakrabarti *et al.*, 1972). It can interact with the translocase enzyme which blocks mRNA translocation on cytosolic (but not organellar) level (Obrig *et al.*, 1971; Setkov *et al.*, 1992; Suzuki *et al.*, 1992). Cycloheximide is also broadly used for the degradation kinetics of a given protein. It is also reported that cycloheximide can sometimes disrupt cellular metabolism other than by inhibiting protein synthesis (Ellis and Macdonald, 1970). We speculated that GCL protein may respond to cycloheximide perturbance, therefore CHX effect was investigated in *Arabidopsis* seedlings grown in liquid culture. Interestingly, as is shown in Figure 15 (under non-reducing conditions), a shifting from oxidized GCL to reduced GCL was observed by increasing the incubation time with cycloheximide, especially at the time point of 48h treatment, protein largely appeared in the reduced form. Moreover, CHX-treated GCL proteins always behaved in a more reduced manner compared with those of H_2O-treated control. However, we also noticed some additional bands shown near reduced bands. What are these bands and how cycloheximide may play a role remain to be further explored.

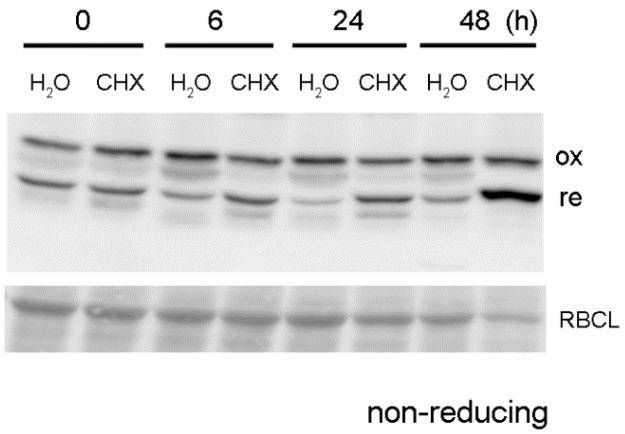

Figure 15. Redox sensitivity of GCL by cycloheximide (CHX) treatment

Arabidopsis seedlings were grown in liquid culture in the shaker under continuous light conditions for 10 days. Then 100μM cycloheximide or H_2O were added to the media for 0h, 6h, 24h or 48h. Seedlings were harvested at each time point. After protein extraction, samples were separated by polyacrylamide gel electrophoresis for western blot analysis. The oxidized and reduced GCL were labelled with ox and re, respectively. GCL redox profiles were determined under non-reducing conditions. The lower panel shows the loading control (the large subunit of Rubisco (RBCL)) of protein amount by amido black staining.

3.7. Redox-dependent control of MAPK phosphatase 2 (MKP2)

The studies on tobacco MAPKs (namely WIPK and SIPK) have found that high glutathione levels can cause the sustained activation of WIPK and SIPK (Matern *et al.*, 2015). Similarly, the increased MAPK activities were also shown in the *Arabidopsis cat2-1*, the mutant which is deficient in catalase but contains the enhanced gluthathione levels. In addition, the *Arabidopsis* MPK2 can be glutathionylated *in vitro* at the Cys109 in the active site (personal communication with Tatjana Peskan-Berghöfer and Sanja Matern). Based on these findings, it might be assumed that MKP2 undergoes modification or degradation under oxidative stress or high-level GSH conditions.

To investigate the regulation of MPK2 in response to oxidative stress, the *Arabidopsis* myc:MKP2-inducible lines were generated. As shown in Figure 16, the expression profiles in these different lines were examined by Western blot analysis with anti-myc antibodies. The expression of myc:MKP2 protein in seedlings was induced by dexamethasone treatment. Some lines had low level of myc:MKP2 expression even without dexamethasone treatment, however, some lines exerted strong induction without background (e.g. 12-3-3 and 16-7-5) and were used for the later studies.

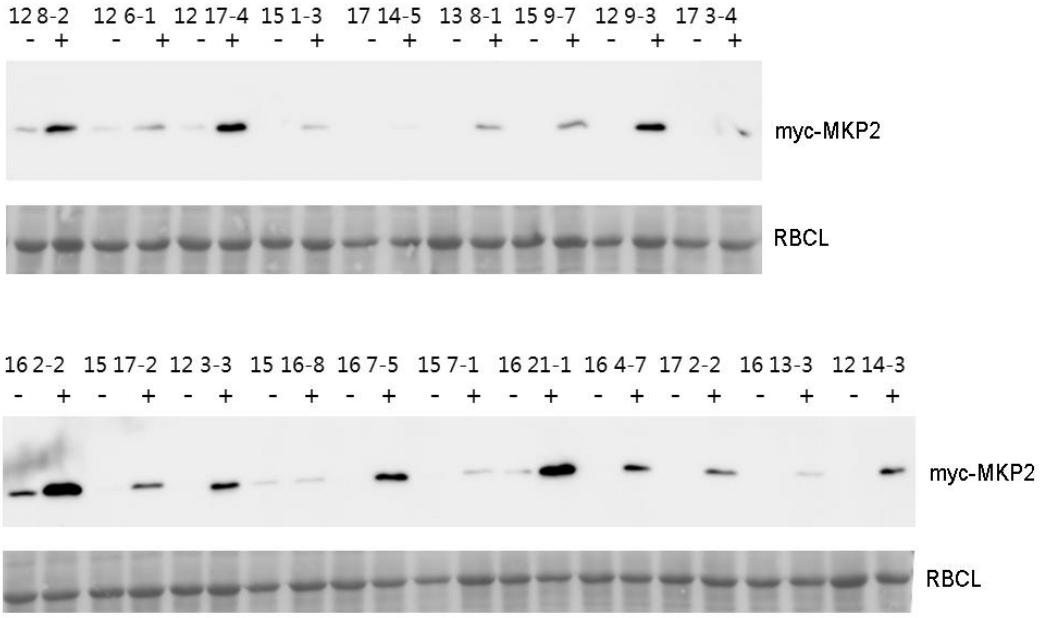

Figure 16. Expression profiles of dex-inducible myc:MKP2 constructs in transgenic *Arabidopsis* lines

Numbers above represent different lines examined. The symbols minus (-) and plus (+) stand for without and with dexamethasone treatment, respectively. The large subunit of Rubisco (RBCL) indicates the loading control.

To gain a further knowledge on redox regulation on MKP2 protein, we treated *Arabidopsis* seedlings expressing myc:MKP2 with 20mM H_2O_2. Figure 17 shows that within one hour, MKP2 accumulation is similar in treated and non-treated samples; however, MKP2 amount in the samples treated with H_2O_2 for 18h is abviously lower than in those without treatment. MPK3, the target of MKP2 dephosphorylation, is rather stable during the whole time period no matter the tissue has been treated with H_2O_2 or not. It reveals that the MKP2 protein accumulation is affected under conditions of sustained oxidative stress.

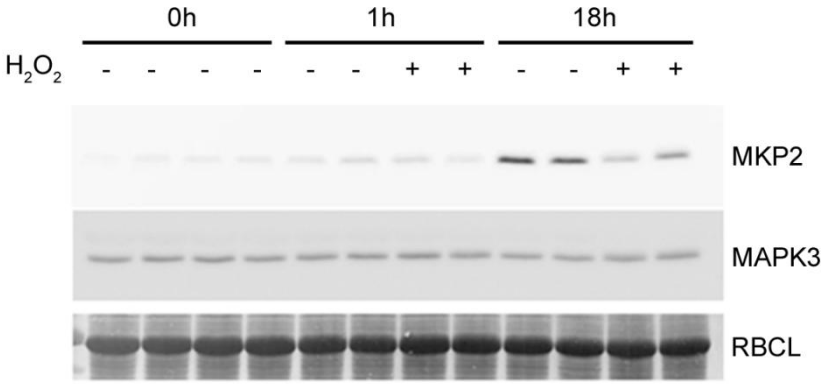

Figure 17. myc:MKP2 protein accumulation upon H_2O_2 treatment

14 days old seedlings of *A. thaliana* inducible line 12-3-3 were grown under standard conditions. Whole seedlings were used for H_2O_2 treatment in 24-well plates. Protein expression has been induced by dexamethasone. 6 h later, 20mM H_2O_2 has been added to monitor protein turn-over. The samples have been collected 1h and 18 h after H_2O_2 treatment. Proteins were extracted with 1 x SDS-loading buffer (5 µl/mg fresh weight) and same volumes were loaded. Samples were separated on SDS-PAGE and subjected to immunoblot analysis. The large subunit of Rubisco (RBCL) indicates the loading control.

4. Discussion

4.1. Mutant GCL proteins reveal several amino acid residues responsible for dimerization

Crystal structure has been resolved for GCL in *Brassica juncea* which is arranged as dimer (Hothorn *et al.*, 2006). The dimer interface is shown to contain 11 amino acid residues, among which several salt bridges and aromatic amino acid side chains are highlighted for their contribution of the zipper-like contact zone (Hothorn *et al.*, 2006). It is noteworthy that amino acid residues in the region of the dimer interface are highly conserved for all GCL sequences in higher plant species and only little changes were observed (Gromes *et al.*, 2008). In addition, previous catalytic studies demonstrated that the plant GCL activation depends on formation of the regulatory intramolecular disulfide bridge and the subsequent formation of homodimers (Gromes *et al.*, 2008; Hicks *et al.*, 2007; Hothorn *et al.*, 2006). Based on this knowledge, we thereby evaluated the contribution of dimerization of GCL in *Arabidopsis* through mutagenesis. Substitution of amino acid residues was designed to maintain their similarity in size and structure in order to minimize the protein conformation perturbation, but electric charges have been abolished since they define the interaction between amino acid residues. The use of size exclusion chromatography confirmed that, unlike wild-type GCL, the generated mutants were unable to dimerize, as a shift of elution profiles was observed (Figure 6). In the mutant protein Glu141/Arg403, an arginine residue replaced with a glutamate residue abolished the formation of the salt bridge. In addition, substitution of tyrosine for leucine in the mutant Tyr194/Phe483 disrupted hydrophobic interactions in the dimer interface. These findings suggested that two types of interactions, salt bridges and hydrophobic interactions, are important for dimerization. Single amino acid replacement was sufficient to disrupt dimer formation,

highlighting the importance of conserved amino acid residues, including Glu141, Arg403, Glu201 and Tyr194, for the dimerization of the GCL protein. We fail to purify the mutants replacing Phe143 and Lys479, indicating that mutation at these positions might have changed the overall structure and resulted in protein aggregation.

4.2. Influencing factors for dimer-monomer transition

4.2.1. Influence of ionic strength

The fact that WT AtGCL acts as a dimer, which can be disrupted by reducing agents, whereas mutants form a monomer, has prompt us to investigate the possible influence of different factors on dimer-monomer transition. The effect of ionic strength on protein dimerization have been reported for proteins such as β-lactoglobulin (Aymard *et al.*, 1996). Aran *et al.* (2008) showed that increasing amounts of Mg^{2+} enhance peroxidase oligomerization. In our study, the characterization of the influence of the ionic strength was carried out by gel filtration. Only partial oxidized WT AtGCL proteins dissociated into monomers at low ionic strength (Figure 7). This shift may be explained by ionic strength impacting on geometry of the dimer. Possibly, decreasing ionic strength destabilize the interface by repulsive interactions. Based on our observation, we suggest that under physiological conditions, in particular, at the high ionic strength of chloroplast stroma (~100-200 mM), GCL can be in the dimer form and will dissociate into monomer quickly only after reduction of its regulatory disulfide bridge (CC2).

4.2.2. Influence of pH

Arndt *et al.* (1998) revealed the variation of pH had a dramatic influence on the conversion rate of dimer to monomer in antibody single-chain Fv fragments. Dynein

light chain protein behaves as a homodimer at physiological pH, but dissociation occurs when pH value is less than 4.5 which can be explained by electric charge repulsion leading to dimer dissociation (Barbar and Hare, 2004; Barbar *et al.*, 2001; Mohan *et al.*, 2009). Diakonova *et al.* (2016) demonstrated the rate of ferredoxin-FNR complex formation is constant in a wide range of physiologically significant pH values, whereas ferredoxin–hydrogenase complex formation is greatly influenced by pH. However, our results presented here show that there is pH variation did not change the dimer state for WT AtGCL (Figure 8). It suggests the GCL is presumably stable within small pH variation, although we cannot yet rule out the possibilities that GCL profiles change when applying broader pH variation, as titratable groups might exist in the interface. Indeed, the impact of pH on dimer/monomer state is not easy to rationalize and may differ among proteins. So there is no surprise to find some different reports (Mohan *et al.*, 2009).

4.2.3. Dimer formation is dependent on protein concentration

Besides external factors such as ionic strength and pH mentioned above, the conversion between dimer and monomer is also sensitive to the absolute concentration of GCL. This is supported by the evidence that decreasing the concentration of recombinant GCL results in dimer transition into monomer (Figure 10C-E). This is consistent with followed result of immunoblotting after SDS-PAGE under non-reducing conditions (Figure 10F-H). Furthermore, native PAGE analysis of GCL dilution series showed band changes (Figure S 3), presumably representing dimer-monomer transition irrespective of additional bands detected nearby.

Moreover, FPLC experiments presented in Figure 10C-E displayed dissociation into monomers at concentrations below 10^{-6} M. We also tried to verify this estimation and measure the specific dissociation constant by isothermal titration calorimetry (ITC), unfortunately, it was not successful due to lack of sensitivity at very low concentration range. However, ITC measurements at higher GCL concentration indicated that

dimers may associate to form tetramers, albeit with much lower affinity (Kd: 9 x 10^{-5} M; Figure 13). Besides ITC method, there are also several approaches which can be used to determine the dissociation constant, including optical ratiometric based system as well as measuring fluorescence intensity or ratio by FRET (Lichten and Swain, 2011; Pomorski *et al.*, 2013). These analytical methods are currently the focus of interest in biochemical studies.

As GCL is exclusively localized in plastids (Wachter *et al*., 2005), a reliable assessment of its concentration in this compartment is favorable to answer the question whether oxidized GCL protein dimerizes *in vivo,* since dimerization depends on protein concentration. Based on the theory derived from previous studies that plastid volume represents not more than 10 % of total tissue volume, and on our observations from the immunological quantification of GCL protein (Figure 12), it is predicted that a plastidial concentration of GCL in *Arabidopsis* is about 5 x 10^{-3} M. Considering the estimated dissociation concentration below 10^{-6} M, oxidized GCL protein is expected to be entirely dimerized at this concentration (Figure 10C-E). Whether these results from *in vitro* experiments bear any relationship to the situation under physiological conditions is an open question.

4.2.4. Reversibility of the dimerization correlates with redox state

Association equilibrium is also very much dependent on the intramolecular disulfide bond. This is supported by the observation that reduction of the conserved intramolecular disulfide bridge by reducing agent is coupled to disruption the GCL dimer, resulting in reduced enzyme activity (Gromes *et al.*, 2008; Hicks *et al.*, 2007; Hothorn *et al.*, 2006). It is also verified in the present study (Figure 6), that the FPLC elution profile of WT GCL shifts upon the addition of the reducing agent DTT, and no effect of reduction was observed on GCL mutants since their dimer formations were disrupted. The redox regulation of plant GCL involves two intramolecular disulfide

bonds (Hothorn *et al.*, 2006). Reduction of CC1 induces structural changes and block substrates accessibility, however, the second disulfide bridge CC2 maintains a dimeric state of oxidized GCL. Characterization of 2-CysPrx demonstrates that its reduced form exists as decamer, while the oxidized form tends to form a dimer (Barranco-Medina *et al.*, 2009). This redox dependence of oligomerization associates with 2-CysPrx compartmentation and function in response to cellular changes. In addition, Chauhan and Mande (2001) reported that in the alkyl hydroperoxidase AhpC, dimerization of individual subunits occurs through an intersubunit disulfide bond formation. These studies all point to the importance of redox control in the oligomeric state of proteins. However, there is still very little knowledge of the nature of protein transition. To this end, further biochemical investigations are needed to advance our understanding.

4.3. Multilayer regulation on GCL activity

4.3.1. GCL activity results from the formation of disulfide bond rather than from dimerization

Previous studies reveal the GCL activation is triggered by intramolecular disulfide bond formation followed by homodimerization (Gromes *et al.*, 2008). Based on this knowledge, in this study, the contribution of dimer formation to GCL activation was evaluated in enzyme activity assay (Figure 9). GCL activities were measured when WT GCL was in the oxidized dimeric state and mutant GCL proteins in the monomeric state. The redox states of WT GCL and mutants were demonstrated in Figure 5, the ratio of oxidized/reduced form among protein variants behaved differently under non-reducing conditions. By comparing enzyme activities of different recombinant GCL variants, we came to the conclusion that disruption of dimerization does not have the significant impact on specific activity, indicating the activation of GCL enzyme is

predominantly attributed to the formation of the regulatory intramolecular disulfide bridge (Cys186/Cys406). It is in accordance with the reduced activities observed in GCL WT and mutants upon DTT treatment (Figure 9). If a more reduced potential is favored in the subcellular context, then GCL activation is attenuated. The estimation of redox midpoint potential also indicates that AtGCL behaves as a redox-active protein (Hicks *et al.*, 2007).

4.3.2. Substrates and GSH regulation on GCL

Substrate availability plays a critical role in GCL activation. In comparison with substrate glutamate and ATP, cysteine controls the GCL protein in a more decisive way. The K_m values measured in this study are consistent with previously reported data which are close to the cellular concentrations (Hell and Bergmann, 1990; Hothorn *et al.*, 2006) (Table 2). It is noteworthy that K_m values in mutants are in the similar range compared with those in wild type GCL, indicating the dimer formation has little impact of substrate affinity on GCL enzyme. As supply with S was demonstrated in relation to their ability for GSH accumulation (Noctor *et al.*, 2002; Srivastava and D'souza, 2009), together with the evidence that cysteine concentration is elevated in *Arabidopsis* plants which display altered GCL activity (Vernoux *et al.*, 2000), it is conceivable that the limitation of GCL activity by cysteine availability is of particular significance in controlling GSH biosynthesis.

4.3.3. Other possibilities for GCL regulation

Up to date, the post-translational regulation of plant GCL remains largely unexamined. However, studies from mammalian cells have shown that protein phosphorylation can serve as one regulatory way for GCL activation (Wei-Min *et al.*, 1996). In animals, GCL was shown to be deactivated by phosphorylation via protein kinases, as applying of phosphatase inhibitors *in vitro* blocked the activation of GCL probably through

dephosphorylation (Toroser and Sohal, 2005). Phosphorylation-dephosphorylation may play a role in modulation of GCL protein. Nevertheless, this has not been reported in plants. It will be of interest to investigate whether phosphorylation mechanisms also fit into plant GCL. In addition, signal transduction related compounds may also exert regulatory influence on GCL activation. Kinetic analysis of GCL in *Drosophila* extracts demonstrates that the activity of GCL is greatly enhanced by NADPH, which is linked to GSH recycling (Toroser *et al.*, 2006). It is postulated that specific binding of ligands, such as NADPH, may exemplify another potential mechanism for eukaryotic GCL regulation (Toroser and Sohal, 2005).

4.4. Oxidative stress and redox state of GCL

Recent studies have found oxidative stress causes shifting of redox state in GCL protein both *in vivo* and *in vitro* (Hicks *et al.*, 2007; Hothorn *et al.*, 2006; Jez *et al.*, 2004). A more oxidized form was observed in *Arabidopsis* seedlings in response to hydrogen peroxide treatment (Hicks *et al.*, 2007). Similar experiments have been performed in this study (Figure 14), and we extended the treatment time to up to 24 hours to evaluate the long-time effect of H_2O_2. The GCL oxidation induced within the short time (5h) seems to be attenuated after long-time (24h) exposure. It might be assumed that the cellular perturbation triggered by moderate H_2O_2 is diminishing through the timeline, and after a while the redox-active GCL is recovered back to the physiological state. The results presented here show that H_2O_2 induce GCL oxidation within the short time range. It is suggested that the plant GCL is sensitive to redox changes induced by H_2O_2, although no effect is shown at the transcriptional level (Meyer and Fricker, 2002; Xiang and Oliver, 1998).

Other oxidative stresses were also reported to impact on the redox state of GCL. Exposing *Arabidopsis* to heavy metal cadmium induces GCL oxidation (Hicks *et al.*, 2007). Buthionine sulfoximine (BSO) specifically inhibits GCL activity and causes oxidative stress through the decreased capacity to synthesize GSH (Griffith and

Meister, 1979; Jez *et al.*, 2004; Maughan *et al.*, 2010). In addition, GCL seems to be responsive to proteasome inhibitor cycloheximide (CHX). CHX-treated GCL behaves as more reduced form as compared to the control (Figure 15). This result was not expected since stressful conditions were thought to induce the protein oxidation. However, it is conceivable that CHX might inhibit the cellular metabolism in a way that switch off oxidative stress related signaling pathways.

Our results indicate that, like other redox-responsive proteins such as glutathione reductase and superoxide dismutase (Herouart *et al.*, 1993), GCL protein senses cellular redox changes and reacts to oxidative signals by adjusting redox state. However, there is very little knowledge of the molecular mechanism controlling the distribution of GCL between oxidized and reduced forms. It has been predicted that thioredoxin or glutaredoxin may play a crucial role since the thioredoxin and glutaredoxin systems are found in the chloroplast stroma where GCL resides (Rouhier *et al.*, 2008).

4.5. What is the function of dimerization?

Considering the evidence that following redox activation, the dimerization occurs in plastids due to high GCL concentration, as well as the observation that the dimer formation has little contribution to enzyme activity, it is an open question what is the physiological role of GCL dimerization.

It is assumed that the dimer formation is confined to the plant GCLs, whereas proteobacteria GCLs behave only as monomers, although they share extensive sequence similarity with plant GCLs. In addition, plant GCLs differ from those from mammalian cells with regard to structural properties. It is likely that dimer-monomer transition upon redox activation is a unique feature of plants related to adapting plastidial environment (Gromes *et al.*, 2008).

Previous studies have suggested that the homodimer formation is related to protein stabilities (Messaritou *et al.*, 2009). As GCL activation is triggered by oxidative stress

which also induces the enhanced proteolytic activity in plastids, it is conceivable that GCL dimerization might play a role in controlling protein stabilization. Additionally, several other reports imply that dimerization mediates signal transduction, transcriptional regulation, ER export and ligand binding (Angers *et al.*, 2002). However, these speculations need to be further verified by *in vivo* studies. GCL transgenic and knock-out lines will facilitate the functional analysis of GCL dimerization. Our first attempt was made to generate redox-insensitive CC2 mutant in *Arabidopsis*. Taken together, examining the molecular basis of GCL regulation is just at an early stage.

4.6. Redox regulation on *Arabidopsis* MAPK phosphatase 2 (MKP2)

MAPK pathways contain a set of molecular control networks that modulate multiple physiological processes. In recent years, it has been found that MAKPs are involved in stress responses. As MKP2 dephosphorylates AtMAPK3 and AtMAPK6, it indicates a MKP2 is a part of the mechanism involved in MAPK signaling pathways in the regulation of stress responses. The MKPs act as a switch that determines the MAPK activation.

The results from the present study demonstrate that sustained oxidative stress affects MKP2 protein accumulation, suggesting MKP2 is a potential target for H_2O_2-induced oxidation. It is possible that MKP2 degrades upon oxidative stress. This could be further investigated by blocking the protein translation (CHX treament) and monitor MKP2 stability in response to oxidative stress. The Cys residues in proteins are subject to various redox-dependent modifications in ROS signaling. The Cys109 of MKP2 is necessary for phosphatase activity and it is conserved among all MKPs from the plant and animal origin. It is assumed that oxidation stress affects MKP2 by modifying the Cys109.

Evidence has emerged that MAPKs can be activated in a glutathione-dependent manner. Transient activation of MAPKs in tobacco and *Arabidopsis* is related to increased glutathione biosynthesis (Matern *et al.*, 2015). It might be proposed that this regulation occurs at the level of MKP2, since it plays a pivotal role in MAPK signaling. In addition, MKP2 can be glutathionylated *in vitro*, therefore it may be speculated that endogenous MKP2 undergoes protein modifications under stress conditions. This assumption could be verified by mass spectrometry.

Following this study, on one hand, the redox-dependent activity of MKP2 could be examined using immunoprecipitated myc:MKP2 from inducible *Arabidopsis* lines. On the other hand, it would be interesting to examine the MPK2 stability in *cat2-1* mutant, as elevated glutathione content in *cat2-1* mutant may play a role in the regulation of MKP2.

5. Materials and methods

5.1. Plant materials and cultures

5.1.1. Plant cultivation

Arabidopsis thaliana (ecotype Columbia (Col-0) and transgenic lines) and *Nicotiana tabacum* were cultivated on ½ MS agar medium and MS agar medium (Serva), respectively. The plants were grown in a climate chamber at 25°C under 16 hours (long-day) light period (100-200 µmol m^{-2} s^{-1}) for two weeks. If needed, the seedlings were further transferred to the soil and grown in the greenhouse under long-day (16 h) conditions at 22°C.

For *Arabidopsis* liquid culture, the seeds of Col-0 were grown in 250 ml flasks containing the liquid medium. The plants were grown in liquid culture in the shaker under continuous light conditions for 10 days.

The seeds of *Zea mays* were put on a wet filter paper geminated for three days in the dark at room temperature. Afterwards they were grown in a climate chamber at 25°C under 16 hours light period for 5 days.

Murashige & Skoog (MS) agar medium: Murashige & Skoog with vitamins (Duchefa, Haarlem, Netherlands)) (2.2 g/l for ½ MS, 4.4 g/l for MS), 2 % (w/v) Sucrose (Roth), 0.8 % (w/v) Agar (Duchefa), pH5.7

Liquid medium: 4.3 g/l MS basal salt mixture (Duchefa, Haarlem, Netherlands), 0.5 g/l MES, 2 % sucrose, distilled water, pH 5.7

5.1.2. Seeds sterilization

The plant seeds were sterilized in the solution of 1.3% sodium hypochloride (v/v) and

0.01% Tween (v/v) for 3 minutes and washed thoroughly with absolute ethanol three times. Afterwards, seeds were left to dry in the laminar flow cabinet.

5.1.3. Stress treatments

H_2O_2 treatment

For monitoring GCL upon H_2O_2 treatment, *Arabidopsis* seedlings were grown on ½ MS medium for two weeks and treated with H_2O_2 (5mM, 10mM) or H_2O for 0-24 hour. Maize seedlings were also treated with H_2O_2 (5mM, 10mM) or H_2O for 0-24 hour. Root tissue of seedlings was used for analysis. For investigating MKP2 accumulation upon H_2O_2 treatment, 14 days old seedlings of Col-0$^{myc\text{-}MKP2}$ inducible lines were used. For treatment, seedling were transferred into 24-well plates, each well contained 3 seedlings in 1 ml liquid ½ MS. Whole seedlings were used for treatment in 24-well plates. Protein expression was induced by dexamethasone. 6 h later, dexamethasone was removed and 20mM H_2O_2 was added to monitor protein turn-over. The samples have been collected 1h and 18 h after H_2O_2 treatment under long day conditions.

Cycloheximide (CHX) treatment

For analyzing GCL, *Arabidopsis* seedlings grown in liquid culture were treated 100µM cycloheximide or H_2O for 0h, 6h, 24h or 48h in the shaker (120 rpm) under continuous light conditions. Seedlings were harvested at each time point. For analyzing MAPK and MKP2, seedlings of Col-0$^{myc\text{-}MKP2}$ lines, including wild type and mutant version of MKP2 (Cys109 is replaced with Ser), were first induced by dexamethasone for 6 hours, and then either treated with 100 µM CHX alone or 100 µM CHX and 20 mM H_2O_2 were applied together for 19 hours under long day conditions.

5.2. Bacterial stains and cultures

5.2.1. Bacterial strains

For cloning purposes

Escherichia coli DH5α (Invitrogen): F-, φ80lacZΔM15, Δ(lacZYA-argF)U169, recA1, endA1, hsdR17(rk-, mk+), phoA, supE44, thi1, gyrA96, relA1, λ-

Escherichia coli XL1-Blue (Stratagene): recA1, endA1, gyrA96, thi-1, hsdR17, supE44, relA1, lac- (F', proAB+, lacIq, lacZ_M15::Tn10(tetr)

For protein overexpression

Rosetta gami [DE3] (Novagen, Madison, USA): Δ(ara-leu)7697, ΔlacX74, ΔphoA, Pvu II, phoR, araD139, ahpC, galE, galK, rpsLF'[lac+(lacIq)pro], gor522 ::Tn10, trxB ::kan, pRARE

5.2.2. Bacterial media and culture conditions

Antibiotics used for plasmids selection

Ampicillin: 100µg/ml dissolved in H_2O, stock: 100mg/ml

Chloramphenicol: 34µg/ml dissolved in EtOH, stock: 34mg/ml

Bacterial media

Low Salt Luria Bertani (LS-LB)-medium:

10 g/l tryptone, 5 g/l yeast extract, 5 g/l NaCl, pH 7.0; for plate cultures 2 % (w/v) agar was added to the medium. After autoclaving at 120 °C for 20 min, the media were cooled down to around 50°C and appropriate antibiotics were added.

E. coli was grown at 37 °C in liquid LB medium and shaked at the speed of 200 rpm.

SOC-medium:

20 g/l tryptone, 5 g/l yeast extract, 10 mM NaCl, 2,5 mM KCl, 10 mM MgCl2 , 10 mM MgSO4, 10 mM glucose, pH 7.0

Terrific Broth (TB)-medium:

For 1 liter TB-medium, the following chemicals were used.

100 ml TB1:1.7 mM KH_2PO_4, 7.2 mM K_2HPO_4

900 ml TB2: 2.4% yeast extract, 1.2% tryptone, 4% glycerol

TB1 and TB2 were mixed together after being autoclaved separately.

E. coli was grown at 37 °C in liquid LB medium and shaked at the speed of 200 rpm. After inducing overexpression of recombinant proteins, the temperature was set to 30°C for incubation.

5.2.3. Preparation of glycerol stocks

Glycerol stocks were prepared for long-term storage of bacterial strains. 150 µl 100 % glycerol was added to 600 µl liquid culture, the mixture was then frozen in liquid nitrogen and stored at -80 °C.

5.2.4. Production of bacterial competent cells

The chosen *E.coli* strain was grown in 1 liter LB medium to an OD_{600} 0.7. The culture was cooled down on ice, and then centrifuged at the speed of 1,500 g and 4°C for 5 minutes to harvest the cells. The collected cells were washed two times with 250 ml ice-cold sterile water followed by 20 ml ice-cold sterile 10% glycerol. *E.coli* cells were finally resuspended in 4 ml of 10 % glycerol. Every 50 µl-aliquot was added in 0.5 ml tube, frozen in liquid nitrogen, and stored at -80 °C for later usage.

Transformation efficiency (Et) was estimated by transforming 10 pg of pUC19 plasmid into the competent cells. The colonies grown on LB selective media were counted to fit into the equation: Et = colonies/µg/dilution. The minimum efficiency required was 2 x 10^8 cfu/µg DNA.

5.2.5. Transformation of bacterial competent cells

For transformation by electroporation, 50 µl of *E.coli* competent cells (see 5.2.4) were thawed on ice and 0.5 to 2 µl of plasmid or ligation product was added. The transformation was conducted by electroporation in the BioRad GenePulser II system (BioRad) at 200 W, 1.8 kV and 25 µF. 1 ml SOC medium (see 5.2.2) was quickly added to the *E.coli* cells after electroporation. The cells were then incubated for 1 hour at 37°C and subsequently spread over the LB agar plates.

5.3. Nucleic acid techniques

5.3.1. Isolation of genomic DNA from plants

Isolation of genomic DNA (gDNA) from plant tissue was performed with Edwards' buffer (400 mM LiCl, 200 mM Tris, 25 mM EDTA and 1% (w/v) SDS, pH 9.0). 50 mg leaves from *Arabidopsis* were homogenized in a 1.5 ml eppendorf tube and 500 µl of extraction buffer were added. After mixing the sample by vortexing, it was centrifuged at 11,000 g at 4°C for 5 min. 300 µl of supernatant was transferred into a new tube and 300 µl of 100% isopropanol was added and mixed gently. The sample was centrifuged at 11,000 g for 10 min. The pellet was washed once with 70 % (v/v) ethanol. After the ethanol dried out, DNA was eluted in 25 µl sterile water. The isolated gDNA was used for selecting *Arabidopsis* GCL knock-out lines in which CC2 is mutated.

5.3.2. Isolation of plasmid DNA from bacterial culture

2-4 ml of bacterial overnight cultures were centrifuged at the speed of 15,000 g for 1 min. The collected pellet was used for plasmid DNA extraction with the GeneJET Plasmid Miniprep Kit (Thermo Scientific) according to the manufacturer's instructions.

JETSTAR2.0 Midi Kit (Genomed) was chosen for production of plasmid DNA if higher-yields were necessary.

5.3.3. Determination of nucleic acid concentration

Determination of nucleic acid concentration was conducted spectrophotometrically with the Nanodrop ND-2000 (Peqlab). The absorbance was measured at 260 and 280 nm by application of Lambert-Beer's law. The ratio of OD260/OD280 was used as indication of purity.

5.3.4. Oligonucleotides

All oligonucleotides were synthesized by Eurofins (Munich, Germany). and dissolved in double distilled sterile water or TE buffer (10 mM Tris-base, 1 mM EDTA, pH 8.0) to a final concentration of 100 µM and stored at -20°C. The primers used in this study (Table S 1) were designed by Primer Premier (http://www.premierbiosoft.com/primerdesign/).

5.3.5. Agarose gel electrophoresis

DNA samples were mixed with 5x DNA loading buffer (50% glycerol, 5x TAE buffer, 1% Orange-G). They were loaded on 0.8 or 1% agarose gels in 1x TAE buffer (40 mM tris-base, 20 mM sodium acetate, 1 mM EDTA, pH 7.2). The voltage for gel running was set at 70 to 90 V. GeneRuler DNA ladder was purchased from Thermo Scientific. DNA fragments were stained in 1 mg/l ethidiumbromide and visualized under UV-light using INTAS science imaging instruments (Göttingen, Germany).

5.3.6. Polymerase chain reaction (PCR)

Polymerase chain reaction (PCR) was performed to amplify DNA fragments. The non

proof-reading Taq polymerase (Sigma-Aldrich) and the proof-reading Phusion polymerase (Finnzymes) were used in this study. The standard PCR reaction mixture and the corresponding PCR program (run by Mastercycler from Eppendorf) are listed in Table 3 and Table 4.

Table 3. Standard PCR reaction mixture

5 x Phusion / 10 xTaq buffer	10 / 5
10 mM dNTPs	1
10 µM Primer (forward)	2.5
10 µM Primer (reverse)	2.5
Phusion / Taq polymerase	0.5 /1
Template	Varying
Distilled water	Add up to 50 (µl)

Table 4. Standard PCR program

Initial denaturation	98 °C	30s	
Denaturation	98 °C	10s	30x cycles
Annealing	varying	30s	
Elongation	72°C	1 min/ 1kb	
Final elongation	72 °C	7min	
End	4 °C		

5.3.7. Purification of DNA fragments

DNA fragments were purified using the GeneJET PCR Purification kit (Thermo Scientific) according to the provider's instructions.

5.3.8. Restriction digestion

All restriction digestions were carried out with enzymes from New England Biolabs (NEB) in the recommended buffers and under optimum conditions according to manufacturer's instruction.

5.3.9. Ligation of DNA fragments

For ligation of DNA fragments into plasmids, 1 µl T4-Ligase (NEB) 1 µl plasmid (100 ng), a 3 to10 fold molar excess of insert, 5 µl 2x buffer and water were added to make up to 10 µl reaction mixture. It was then incubated overnight at 4 °C or 1 h at room temperature.

5.3.10. DNA Sequencing

Sequencing of DNA was conducted by Eurofins GmbH and the following results were analyzed by the software Serial Cloner.

5.3.11. Cloning and mutagenesis of *GCL* from *A. thaliana*

AtGCL (GenBank: CAA71075.1) was amplified by PCR from an *Arabidopsis* cDNA library using primer pairs 5'-CATGCCATGGCGGCAAGTCCTCCAACG-3' and 5'-CCGCTCGAGTTAGTACAGCAGCTCTTCGAACACGG-3' (with restriction sites and protective bases underlined). The predicted plastid transit peptide (Table S 2) was excluded in the GCLs of both, WT and mutants. Mutants were generated by using the QuickChange Mutagenesis kit (Stratagene) according to the manufacturers' instructions. The primers are listed in Table S 1. PCR products were verified by DNA sequencing. All sequences were digested with NcoI and XhoI and cloned into the pETM-20 vector (Hothorn et al., 2003) to produce His-tagged proteins fused with thioredoxin to increase solubility.

5.4. Protein techniques

5.4.1. Expression of recombinant protein in *E.coli*

The overnight culture of *E. coli* Rosetta gami DE3 (Novagen) containing the target vector was transferred to 2 liter LB medium (TB was used for producing more proteins) and cultured at 37°C and 180 rpm until the OD_{600} reached 0.6-0.8. Then the cells were induced with 1 mM isopropyl-β-D-thiogalactopyranoside (IPTG). Bacteria cultures were harvested by centrifugation after 4 hours and the cell pellet was stored at -20°C for one day.

5.4.2. Purification of recombinant protein by affinity chromatography

Recombinant protein were purified by affinity chromatography (Qiagen, Valencia, CA). Pelleted cells were resuspended in lysis buffer (50 mM Tris pH 8.0, 250 mM NaCl, 20 mM imidazol). The suspension was centrifuged at 22,000 *g* for 10 min. The supernatant containing protein crude extract was applied to the HiTrapTM chelating column. After 2-hour circulation, the column was washed with washing buffer (50 mM Tris pH 8.0, 250 mM NaCl, 45 mM Imidazol) and the washing fractions were collected as 1 ml per tube. His-tagged proteins were eluted with elution buffer (50 mM Tris pH 8.0, 250 mM NaCl, 400 mM Imidazol) and the eluted fractions were collected as 1 ml per tube. The eluted proteins were dialyzed against buffer (25 mM HEPES pH 7.5, 5 mM $MgCl_2$, 150 mM NaCl) and cleaved overnight with recombinant tobacco etch virus (TEV) protease at 4 °C. A second Ni^{2+} affinity step was performed after dialysis to separate GCL protein from 6x His tagged protease and thioredoxin. The final protein was concentrated by centrifugal filtration (Amicon Ultra-filter Millipore, 30 kDa MWCO).

5.4.3. Protein extraction from plant tissue

For detecting GCL, 50 to100 mg of tissue were ground and mixed on ice with extraction buffer (50 mM HEPES pH 7.5, 1mM EDTA, 2 mM $MgCl_2$, 10 mM KCl, 10 mM ascobate, 10 mM NEM, 1mM PMSF). After vortexing, the homogenate was centrifuged at 15,000 g for 30 min under 4 °C. The supernatant was taken for gel electrophoresis. 2x reducing or non-reducing loading buffer (Roti-Load, Roth) was added to the sample and denatured by heating to 90 °C for 5 min if needed.

For monitoring MAPK activities, 50 to100 mg of tissue were ground and mixed on ice with extraction buffer (50 mm Tris-HCl, pH 7.5, 10 mm $MgCl_2$, 15 mm EGTA, 100 mm NaCl, 2 mm dithiothreitol, 1 mm NaF, 1 mm NaMo, 0.5 mm $NaVO_3$, 30 mm β-glycerophosphate, and 0.1% Nonidet P-40, 1% anti-protease cocktail (P9599; Sigma). and the homogenate was centrifuged twice at 15,000 g for 10 min under 4 °C and supernatant was taken for gel electrophoresis. For this, 3 volumes of supernatant were mixed with 1 volume of 4x reducing loading buffer (Roti-Load, Roth) and denatured by heating at 85 °C for 5 min. For detecting MAPKs and MKP2 stabilities, 50 to100 mg of tissue was grounded and mixed on ice with 1x reducing loading buffer (5 µl buffer/mg FW) and denatured by heating at 85 °C for 5 min.

5.4.4. Determination of protein concentration

Protein concentration was determined by Bradford assay. 250 µl of 1x Bradford solution (Roth) was added to 10 µl sample in a 96-well plate and the absorbance was measured at 595 nm with the BMG Fluostar plate reader. 0.1, 0.2 and 0.4 µg/µl BSA were used to generate the standard calibration curve for calculating the concentration of protein samples.

5.4.5. SDS-polyacrylamide gel electrophoresis (SDS-PAGE)

SDS-PAGE was performed to separate proteins. Stacking gels were prepared with 3.0 ml water, 1.25 ml stacking gel buffer (0.5 M tris-base pH 6.9, 0.4% SDS), 0.75 ml acrylamide-mix (30% acrylamide/ bisacrylamide mix, 37.5:1, SERVA), 60 µl 10% APS and 6 µl TEMED. 12% resolving gels were prepared with 3.5 ml water, 2.5 ml resolving gel buffer (1.5 M Tris-base pH 8.8, 0.4% SDS), 4.4 ml acrylamide-mix (30% acrylamide/ bisacrylamide mix, 37.5:1, SERVA), 45 µl 10% ammonium persulfate (APS) and 10 µl TEMED. The running buffer has the following compositions: 25 mM tris-base, 200 mM glycine, and 0.1% SDS, pH 8.6. The samples were separated at the voltage of 120 V in stacking gels followed by 200 V in resolving gels.

For native gel electrophoresis, the following solutions were used: acrylamide solution (30 g acrylamide and 0.8 g bis-acrylamide, fill up to 100 ml in distilled water), separating gel buffer (1.5 M Tris HCl, pH 8.8), stacking gel buffer (0.5 M Tris HCl, pH 6.8), polymerizing solution (10 % APS in water and TEMED), electrophoresis buffer (3 g Tris base, 14.4 g glycine, fill up to 100 ml in distilled water, pH8.3). The separating gel was prepared by mixing 5.37 ml acrylamide solution, 3.3 ml separating gel buffer, 4.73 ml water, 90 µl 10% APS and 16 µl TEMED. The stacking gel was prepared by mixing 1.13 ml acrylamide solution, 0.72 ml stacking gel buffer, 2.61ml water, 45 µl 10% APS and 9 µl TEMED. The gel was run at 80 V on ice for 2.5 hours.

5.4.6. Coomassie staining

Coomassie staining was performed after SDS-PAGE to visualize proteins on the gel. The gel was incubated in the staining buffer (0.2% Coomassie Blue G250, 45% methanol, 10% glacial acetic acid) for 30 min and washed with distilled water overnight for destaining.

5.4.7. Immunoblotting

Proteins were transferred to a PVDF membrane (Immobilon P, Millipore) after SDS-PAGE,according to manufacturers' instructions for the membrane. Prior to transfer, the membrane was pretreated with 100% methanol for 20 s, washed with water for 2 min and incubated with blotting buffer (48 mM Tris-base, 39 mM glycine, 20% methanol, 0.0375% SDS) for 5 min. The transfer was performed by a PerfectBlue Semi-Dry Electroblotter (Peqlab) at 25 V and 400 mA for 45 min. Afterwards, the membrane was incubated with 1x TBST buffer (20 mM Tris-base, 150 mM NaCl, 0.05% Tween20) containing 5 % milk powder for 1 hour with shaking. The membrane was washed with 1x TBST buffer five times and incubated with specific primary antibody (diluted according to the Table 5) overnight at 4°C, followed by the same washing step with 1x TBST buffer. The incubation with the secondary antibody was carried out in 1x TBST containing 1 % milk powder at dilution of 1:20000 for 1 h and the membrane was washed with 1x TBST buffer five times. For chemiluminescent detection, Super Signal West Dura Extended Duration Substrate (Thermo Scientific) was used and the protein signals were detected by ImageQuant LAS 4000. Amido black staining solution (0.1% amido black, 45% methanol, 10% glacial acetic acid) was used for membrane staining to visualize the proteins as a loading control.

Table 5. List of primary antibodies

primary antibodies	dilution	solution	sourse
anti-pTEpY (for MAPKp)	1:20000	5 % (w/v) BSA, 0.1 % Tween 20 in 1x TBS	rabbit
anti-MAPK3	1:5000	1 % BSA in TBST	rabbit
anti-myc (for MKP2)	1:10000	2 % BSA in TBST	mouse
anti-GCL	1:5000	1 % milk powder in TBST	rabbit

5.4.8. Enzymatic Characterization of GCL Protein

Specific activities of recombinant AtGCL (WT and mutants) were analyzed in a coupled enzymatic assay as described previously (Abbott *et al.*, 2001). A reaction mixture (0.5 ml) contained reaction buffer (100 mM MOPSO pH 7.0, 150 mM NaCl, 20 mM $MgCl_2$), 10 mM L-cysteine, 20 mM sodium glutamate, 5 mM ATP, 2 mM phosphoenolpyruvate, 0.27 mM NADH, 5 units of type II rabbit muscle pyruvate kinase, and 10 units of type II rabbit muscle lactic dehydrogenase. Reactions were started by adding WT or mutant GCL protein (50 µg). OD_{340} values were measured for calculating the enzyme activites.

For determination of K_m values, different substrate concentrations were applied. K_m for cysteine were determined at 20 mM ATP and 80 mM glutamate, respectively, for ATP at 20 mM cysteine and 80 mM glutamate, respectively, and for glutamate at 20 mM cysteine and 20 mM ATP, respectively. Kinetic parameters were calculated according to v =[S]/(Km +[S]) in GraphPad Prism.

Student's T-test was performed for significance. Results were obtained from three independent experiments and are expressed as means ± standard error (S.E.).

5.4.9. Size-exclusion chromatography (SEC)

Oligmerization state of GCL (WT and mutants) was determined by size-exclusion chromatography (SEC) using a HiLoad 16/600 Superdex 200 pg column (GE Healthcare). The buffer containing 25 mM HEPES (pH 7.5), 5 mM $MgCl_2$ and 150 mM NaCl was used as running buffer and was pre-loaded onto the column. For low-ionic strength solution, 10 mM NaCl was used. The protein was dialyzed with the running buffer overnight and 1 ml sample (50 µg) was loaded onto the column. The elution was conducted at 1 ml/min. 120 mM dithiothreitol was added to the protein if needed. The Superdex 200 column was calibrated with the high and low molecular weight gel filtration calibration kits (GE Healthcare). The calibration curve (Figure S 2) was

generated by the gel phase distribution coefficient (Kav) versus logarithm of the molecular weight (Log Mr). Kav = (Ve - Vo) / (Vc - Vo) where Ve = elution volume, Vo = column void volume (45.39 mL), Vc = geometric column volume (120 mL).

5.4.10. Isothermal titration calorimetry (ITC)

Isothermal titration calorimetry (ITC) was performed to determine the dissociation constant (Kd) of GCL. The protein was dialyzed in the ITC buffer containing 25 mM Hepes (pH 7.5), 150 mM NaCl, and 5 mM $MgCl_2$. The experiment was carried out by a MicroCal PEAQ-ITC machine (Malvern Instruments) at 20 °C according to the manufacturer's instructions. WT AtGCL (450 µM) in the syringe was titrated into the sample cell containing ITC buffer. The MicroCal PEAQ-ITC Analysis Software (Malvern Instruments) was used for data analysis.

5.5. Bioinformatic analysis

The sequence information (DNA and proteins) used in this study was obtained from the NCBI database (http://www.ncbi.nlm.nih.gov/). Protein sequences of GCL from *Nicotiana tabacum*, *Brassica juncea* and *Arabidopsis thaliana* were aligned using Clustal Omega (https://www.ebi.ac.uk/Tools/msa/clustalo/) (Figure S 1). ChloroP 1.1 Server was used for prediction of GCL transit peptide (http://www.cbs.dtu.dk/services/ChloroP/) (Table S 2).

6. Supplements

Table S 1. Primers used for cloning

Original amino acid residues	Mutated amino acid residues	Sequences (5'-3')
E141/R403	K141/R403-5PCR	CATGCCATGGCGGCAAGTCCTCCAACG
		TCCCATTCAAATCTCTTAGCGATACC
	K141/R403-3PCR	CTTCTTAATGGTATCGCTAAGAGATTTG
		CCGCTCGAGTTAGTACAGCAGCTCTTCGAACACGG
	E141/E403-5PCR	CATGCCATGGCGGCAAGTCCTCCAACG
		CACACAGCCTTTCCCAGGGACCTC
	E141/E403-3PCR	GAGGTCCCTGGGAAAGGCTGTGTG
		CCGCTCGAGTTAGTACAGCAGCTCTTCGAACACGG
Q141/M403	Q141/M403-5PCR.1	CATGCCATGGCGGCAAGTCCTCCAACG
		TCCCATTCAAATCTCTGAGCGATACC
	Q141/M403-3PCR.1	TCTTAATGGTATCGCTCAGAGATTTGAATG
		CCGCTCGAGTTAGTACAGCAGCTCTTCGAACACGG
	Q141/M403-5PCR.2	CATGCCATGGCGGCAAGTCCTCCAACG
		ACACAGCCTCATCCAGGGACCTC
	Q141/M403-3PCR.2	AGGTCCCTGGATGAGGCTGTGTGC
		CCGCTCGAGTTAGTACAGCAGCTCTTCGAACACGG
E201/K479	K201/K479-5PCR	CATGCCATGGCGGCAAGTCCTCCAACG
		CCAATTCCCATTTCCTTAGCAACTGCTTTTAC
	K201/K479-3PCR	TCAGGTAAAAGCAGTTGCTAAGGAAATGG
		CCGCTCGAGTTAGTACAGCAGCTCTTCGAACACGG

	E201/E479-5PCR	CATGCCATGGCGGCAAGTCCTCCAACG
		AACCGGCTTCTTCGTAGCCTCTGCG
	E201/E479-3PCR	CAGAGGCTACGAAGAAGCCGGTTTC
		CCGCTCGAGTTAGTACAGCAGCTCTTCGAACACGG
Q201/M479	Q201/M479-5PCR.1	CATGCCATGGCGGCAAGTCCTCCAACG
		CAATTCCCATTTCCTGAGCAACTGCTTTTAC
	Q201/M479-3PCR.1	AGGTAAAAGCAGTTGCTCAGGAAATG
		CCGCTCGAGTTAGTACAGCAGCTCTTCGAACACGG
	Q201/M479-5PCR.2	CATGCCATGGCGGCAAGTCCTCCAACG
		CGGCTTCCATGTAGCCTCTGCG
	Q201/M479-3PCR.2	TAGAGCGCAGAGGCTACATGGAAGC
		CCGCTCGAGTTAGTACAGCAGCTCTTCGAACACGG
F143/W402	L143/W402-5PCR	CATGCCATGGCGGCAAGTCCTCCAACG
		ACTTTTTCCCATTCCAATCTTTCAGC
	L143/W402-3PCR	GGTATCGCTGAAAGATTGGAATGG
		CCGCTCGAGTTAGTACAGCAGCTCTTCGAACACGG
Y194/F483	L194/F483-5PCR	CATGCCATGGCGGCAAGTCCTCCAACG
		GCTTTTACCTGCAAAAGATGTGAATTGACT
	L194/F483-3PCR	GAAGTCAATTCACATCTTTTGCAGGT
		CCGCTCGAGTTAGTACAGCAGCTCTTCGAACACGG

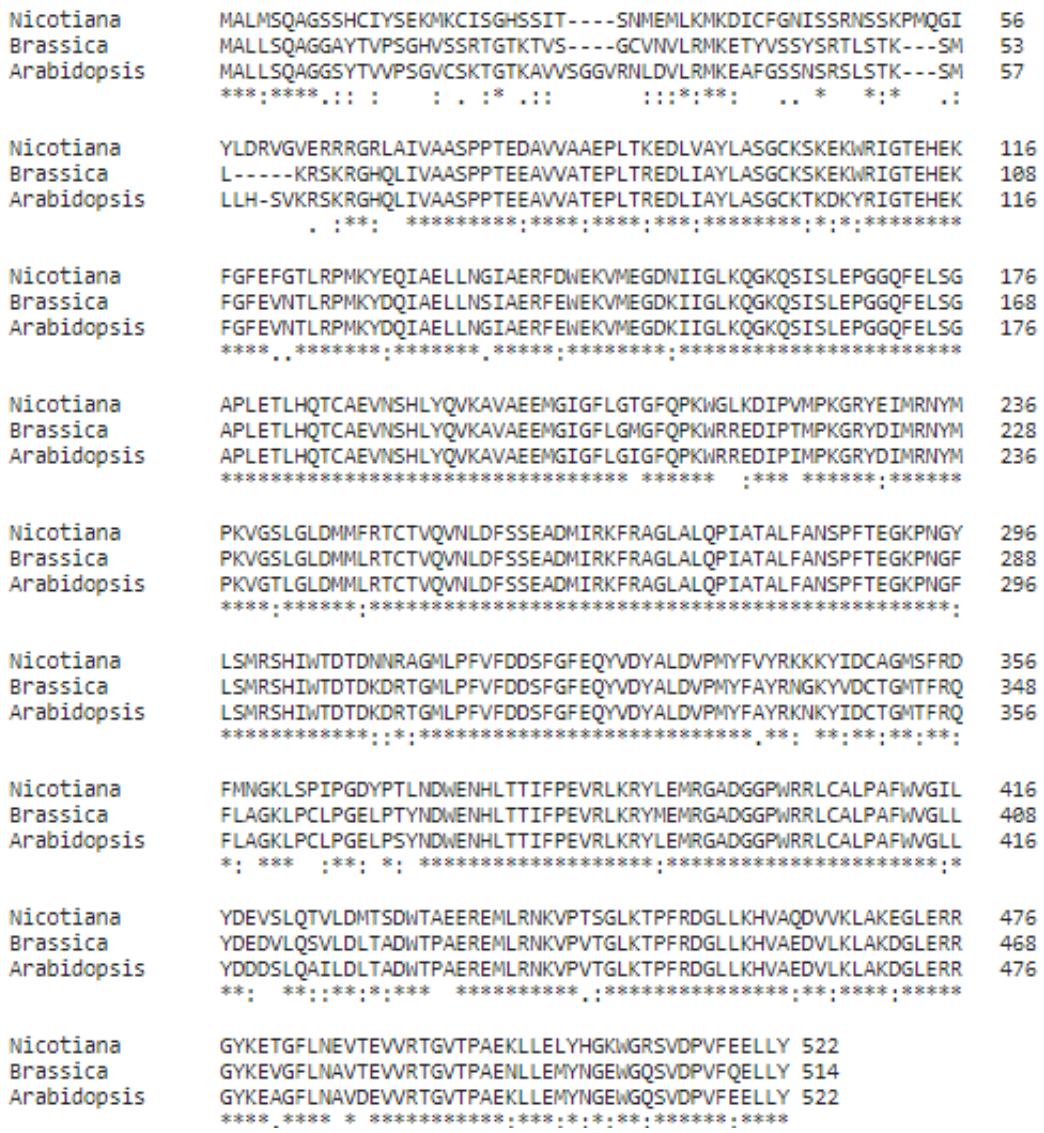

Figure S 1. Sequence alignment of GCLs

Protein sequences of GCL from *Nicotiana tabacum*, *Brassica juncea* and *Arabidopsis thaliana* were aligned using Clustal Omega.

Table S 2. Transit peptide prediction for AtGCL

Name is the name of the submitted sequence. Length is the length of the submitted sequence. Score is the output score from the second step network. The prediction cTP/no cTP is based solely on this score. cTP tells whether or not this is predicted as a cTP-containing sequence; "Y" means that the sequence is predicted to contain a cTP; "-" means that is predicted not to contain a cTP. CS-score is the MEME scoring matrix score for the suggested cleavage site. cTP-length is the predicted length of the presequence. The transit peptide is highlighted in blue in the following AtGCL sequence.

Name	Length	Score	cTP	CS- Score	cTP- length
AtGCL	522	0.558	Y	4.289	73

MALLSQAGGSYTVVPSGVCSKAGTKAVVSGGVRNLDVLRMKEAFGSSYSRSLSTKSMLL
HSVKRSKRGHQLIVAASPPTEEAVVATEPLTREDLIAYLASGCKTKDKYRIGTEHEKFGFE
VNTLRPMKYDQIAELLNGIAERFEWEKVMEGDKIIGLKQGKQSISLEPGGQFELSGAPLET
LHQTCAEVNSHLYQVKAVAEEMGIGFLGIGFQPKWRREDIPIMPKGRYDIMRNYMPKVGT
LGLDMMLRTCTVQVNLDFSSEADMIRKFRAGLALQPIATALFANSPFTEGKPNGFLSMRS
HIWTDTDKDRTGMLPFVFDDSFGFEQYVDYALDVPMYFAYRKNKYIDCTGMTFRQFLAGK
LPCLPGELPSYNDWENHLTTIFPEVRLKRYLEMRGADGGPWRRLCALPAFWVGLLYDDD
SLQAILDLTADWTPAEREMLRNKVPVTGLKTPFRDGLLKHVAEDVLKLAKDGLERRGYKE
AGFLNAVDEVVRTGVTPAEKLLEMYNGEWGQSVDPVFEELLY

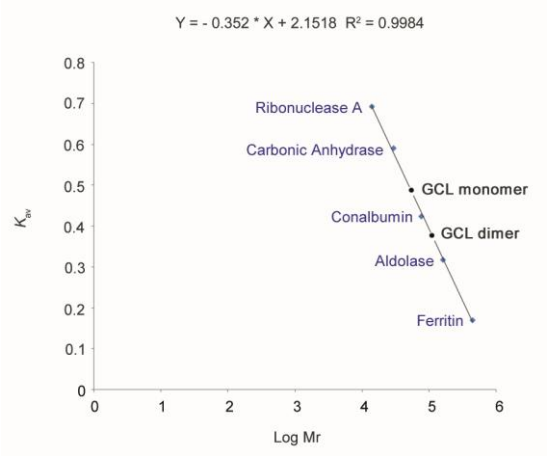

Figure S 2. Calibration curve used to estimate molecular weights for GCLs

Size exclusion chromatography column HiLoad 16/600 Superdex 200 pg was calibrated using Ribonuclease A (13700 Da), Carbonic Anhydrase (29000 Da), Conalbumin (75000 Da), Aldolase (158000 Da), Ferritin (440000 Da). The calibration curve was carried out by the gel phase distribution coefficient (Kav) versus logarithm of the molecular weight (Log Mr). Kav = (Ve - Vo) / (Vc - Vo) where Ve = elution volume, Vo = column void volume (45.39 mL), Vc = geometric column volume (120 mL). The equation, Y = - 0.352 * X + 2.1518 (R2 = 0.9984) was calculated from the calibration curve (straight line) to determine the molecular weight of protein. Blue diamonds on the curve indicate the known calibration standards, black circles correspond to the positions of Kav values for GCL dimer and monomer, the molecular weights of which were estimated to be around 106000 Da and 51000 Da, respectively.

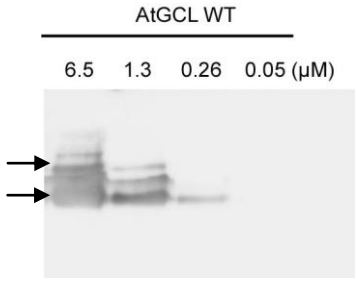

Figure S 3. Immunoblot analysis of recombinant AtGCL WT separated by native PAGE

Different concentrations of recombinant proteins (6.5, 1.3, 0.26 and 0.05 µM) were loaded with same volume in native PAGE for AtGCL WT. The proteins were then subjected to immunoblot analysis using antisera against AtGCL. The proteins behave as dimer and/or monomer indicated by arrow, the additional unspecific bands are observed as well.

7. List of abbreviations

At	*Arabidopsis thaliana*
ADP	adenosine-5'-diphosphate
ATP	adenosine-5'-triphosphate
APS	adenosine-5′-phosphosulfate
APR	APS reductase
Arg	arginine
BSA	bovine serum albumin
Cys	cysteine
CSC	cysteine synthase complex
CC1/CC2	disulfide bridge 1 / disulfide bridge 2
CHX	cycloheximide
DHAR	dehydroascorbic acid reductase
DEX	dexamethasone
DNA	desoxyribonucleic acid
dNTP	desoxyribonucleotide
DTT	dithiothreitol
EDTA	ethylenediamine tetraacetic acid
e.g.	for example
FPLC	fast protein liquid chromatography
FW	fresh weight
g	multiple of standard terrestrial gravity
GSH	glutathione (reduced)
GSSH	glutathione disulfide (oxidized)
GCL	γ-glutamylcysteine ligase
GR	glutathione reductase
GST	glutathione S-transferase

GS	glutathione Synthetase
Gly	glycine
Glu	glutamate
Gln	glutamine
h	hour
HEPES	*N*-(2-Hydroxyethyl) piperazine-2-ethanesulfonic acid
ITC	isothermal titration calorimetry
IPTG	isopropylthiogalactoside
Km	Michaelis Menten constant
Kd	dissociation constant
kDa	kilo daltons
Lys	lysine
min	minute
MES	2-(N-morpholino) ethanesulfonic acid
NCBI	national center for biotechnology information
$NAD(P)^+$	nicotine adenine dinucleotide (phosphate), oxidized
NAD(P)H	nicotine adenine dinucleotide (phosphate), reduced
NEM	*N*-ethylmaleimide
$OD_{x\ nm}$	opticaldensity at x nm wavelength
ORF	open reading frame
Phe	phenylalanine
pH	negative decadic logarithm of hydronium ions
PMSF	phenylmethanesulfonylfluoride
RBCL	rubisco large subunit
rpm	revolutions per minute
ROS	reactive oxygen species
s	second
Ser	serine
SDS	sodium dodecyl sulfate

S.E.	standard error
SEC	size-exclusion chromatography
TEV	tobacco etch virus
TEMED	N,N,N',N'Tetramethylediamine
Tris	2-amino-2-hydroxymethyl-1,3-propanediol (trishydroxymethylaminomethane)
Trp	tryptophan
Tyr	tyrosine
v/v	volume per volume
w/v	weight per volume
WT	wild type
°C	degree celsius

8. References

Abbott JJ, Pei J, Ford JL, Qi Y, Grishin VN, Pitcher LA, Phillips MA, Grishin NV. 2001. Structure prediction and active site analysis of the metal binding determinants in γ-glutamylcysteine synthetase. *Journal of Biological Chemistry* **276**, 42099-42107.

Adachi T, Pimentel DR, Heibeck T, Hou X, Lee YJ, Jiang B, Ido Y, Cohen RA. 2004. S-glutathiolation of Ras mediates redox-sensitive signaling by angiotensin II in vascular smooth muscle cells. *Journal of Biological Chemistry* **279**, 29857-29862.

ADAMS DO, LIYANAGE C. 1993. Glutathione increases in grape berries at the onset of ripening. *American Journal of Enology and Viticulture* **44**, 333-338.

Amir R, Hacham Y, Galili G. 2002. Cystathionine γ-synthase and threonine synthase operate in concert to regulate carbon flow towards methionine in plants. *Trends in Plant Science* **7**, 153-156.

Angers S, Salahpour A, Bouvier M. 2002. Dimerization: an emerging concept for G protein–coupled receptor ontogeny and function. *Annual Review of Pharmacology and Toxicology* **42**, 409-435.

Aran M, Caporaletti D, Senn AM, Tellez de Iñon MT, Girotti MR, Llera AS, Wolosiuk RA. 2008. ATP-dependent modulation and autophosphorylation of rapeseed 2-Cys peroxiredoxin. *The FEBS Journal* **275**, 1450-1463.

Arndt KM, Müller KM, Plückthun A. 1998. Factors influencing the dimer to monomer transition of an antibody single-chain Fv fragment. *Biochemistry* **37**, 12918-12926.

Asada K. 1992. Ascorbate peroxidase–a hydrogen peroxide-scavenging enzyme in plants. *Physiologia Plantarum* **85**, 235-241.

Asada K. 2006. Production and scavenging of reactive oxygen species in chloroplasts and their functions. *Plant Physiology* **141**, 391-396.

Asai T, Tena G, Plotnikova J, Willmann MR, Chiu W-L, Gomez-Gomez L, Boller T, Ausubel FM, Sheen J. 2002. MAP kinase signalling cascade in Arabidopsis innate immunity. *Nature* **415**, 977.

Aymard P, Durand D, Nicolai T. 1996. The effect of temperature and ionic strength on the dimerisation of β-lactoglobulin. *International Journal of Biological Macromolecules* **19**, 213-221.

Bachhawat AK, Thakur A, Kaur J, Zulkifli M. 2013. Glutathione transporters. *Biochimica et Biophysica Acta (BBA)-General Subjects* **1830**, 3154-3164.

Ball L, Accotto G-P, Bechtold U, Creissen G, Funck D, Jimenez A, Kular B,

Leyland N, Mejia-Carranza J, Reynolds H. 2004. Evidence for a direct link between glutathione biosynthesis and stress defense gene expression in Arabidopsis. *The Plant Cell* **16**, 2448-2462.

Barbar E, Hare M. 2004. Characterization of the cargo attachment complex of cytoplasmic dynein using NMR and mass spectrometry. *Methods in Enzymology* **380**, 219-241.

Barbar E, Kleinman B, Imhoff D, Li M, Hays TS, Hare M. 2001. Dimerization and folding of LC8, a highly conserved light chain of cytoplasmic dynein. *Biochemistry* **40**, 1596-1605.

Barranco-Medina S, Lázaro J-J, Dietz K-J. 2009. The oligomeric conformation of peroxiredoxins links redox state to function. *FEBS letters* **583**, 1809-1816.

Bartels S, Besteiro MAG, Lang D, Ulm R. 2010. Emerging functions for plant MAP kinase phosphatases. *Trends in Plant Science* **15**, 322-329.

Bashandy T, Guilleminot J, Vernoux T, Caparros-Ruiz D, Ljung K, Meyer Y, Reichheld J-P. 2010. Interplay between the NADP-linked thioredoxin and glutathione systems in Arabidopsis auxin signaling. *The Plant Cell* **22**, 376-391.

Beck A, Lendzian K, Oven M, Christmann A, Grill E. 2003. Phytochelatin synthase catalyzes key step in turnover of glutathione conjugates. *Phytochemistry* **62**, 423-431.

Bedhomme M, Adamo M, Marchand CH, Couturier J, Rouhier N, Lemaire SD, Zaffagnini M, Trost P. 2012. Glutathionylation of cytosolic glyceraldehyde-3-phosphate dehydrogenase from the model plant Arabidopsis thaliana is reversed by both glutaredoxins and thioredoxins *in vitro*. *Biochemical Journal* **445**, 337-347.

Beinert H. 2000. Iron-sulfur proteins: ancient structures, still full of surprises. *Journal of Biological Inorganic Chemistry* **5**, 2-15.

Benekos K, Kissoudis C, Nianiou-Obeidat I, Labrou N, Madesis P, Kalamaki M, Makris A, Tsaftaris A. 2010. Overexpression of a specific soybean GmGSTU4 isoenzyme improves diphenyl ether and chloroacetanilide herbicide tolerance of transgenic tobacco plants. *Journal of Biotechnology* **150**, 195-201.

Biteau B, Labarre J, Toledano MB. 2003. ATP-dependent reduction of cysteine–sulphinic acid by S. cerevisiae sulphiredoxin. *Nature* **425**, 980.

Cairns NG, Pasternak M, Wachter A, Cobbett CS, Meyer AJ. 2006. Maturation of Arabidopsis seeds is dependent on glutathione biosynthesis within the embryo. *Plant Physiology* **141**, 446-455.

Camps M, Nichols A, Arkinstall S. 2000. Dual specificity phosphatases: a gene

family for control of MAP kinase function. *The FASEB Journal* **14**, 6-16.

Chakrabarti S, Dube D, Roy S. 1972. Effects of emetine and cycloheximide on mitochondrial protein synthesis in different systems. *Biochemical Journal* **128**, 461.

Chauhan R, Mande SC. 2001. Characterization of the Mycobacterium tuberculosis H37Rv alkyl hydroperoxidase AhpC points to the importance of ionic interactions in oligomerization and activity. *Biochemical Journal* **354**, 209-215.

Chen Y-R, Chen C-L, Pfeiffer DR, Zweier JL. 2007. Mitochondrial complex II in the post-ischemic heart oxidative injury and the role of protein S-glutathionylation. *Journal of Biological Chemistry* **282**, 32640-32654.

Chen Y, Shertzer HG, Schneider SN, Nebert DW, Dalton TP. 2005. Glutamate Cysteine ligase catalysis dependence on ATP and modifier subunit for regulation of tissue glutathione levels. *Journal of Biological Chemistry* **280**, 33766-33774.

Cobbett C, Goldsbrough P. 2002. Phytochelatins and metallothioneins: roles in heavy metal detoxification and homeostasis. *Annual Review of Plant Biology* **53**, 159-182.

Cobbett CS, May MJ, Howden R, Rolls B. 1998. The glutathione‐deficient, cadmium‐sensitive mutant, cad2–1, ofArabidopsis thalianais deficient in γ‐glutamylcysteine synthetase. *The Plant Journal* **16**, 73-78.

Colcombet J, Sözen C, Hirt H. 2016. Convergence of multiple MAP3Ks on MKK3 identifies a set of novel stress MAPK modules. *Frontiers in Plant Science* **7**, 1941.

Copley SD, Dhillon JK. 2002. Lateral gene transfer and parallel evolution in the history of glutathione biosynthesis genes. *Genome Biology* **3**, research0025. 0021.

Cummins I, Wortley DJ, Sabbadin F, He Z, Coxon CR, Straker HE, Sellars JD, Knight K, Edwards L, Hughes D. 2013. Key role for a glutathione transferase in multiple-herbicide resistance in grass weeds. *Proceedings of the National Academy of Sciences* **110**, 5812-5817.

Dalle-Donne I, Rossi R, Giustarini D, Colombo R, Milzani A. 2007. S-glutathionylation in protein redox regulation. *Free Radical Biology and Medicine* **43**, 883-898.

Davidian J-C, Kopriva S. 2010. Regulation of sulfate uptake and assimilation—the same or not the same? *Molecular Pant* **3**, 314-325.

De Pinto M, Locato V, De Gara L. 2012. Redox regulation in plant programmed cell death. *Plant, Cell & Environment* **35**, 234-244.

Després C, Chubak C, Rochon A, Clark R, Bethune T, Desveaux D, Fobert PR. 2003. The Arabidopsis NPR1 disease resistance protein is a novel cofactor that

confers redox regulation of DNA binding activity to the basic domain/leucine zipper transcription factor TGA1. *The Plant Cell* **15**, 2181-2191.

Diakonova A, Khrushchev S, Kovalenko I, Riznichenko GY, Rubin A. 2016. Influence of pH and ionic strength on electrostatic properties of ferredoxin, FNR, and hydrogenase and the rate constants of their interaction. *Physical Biology* **13**, 056004.

Díaz-Vivancos P, Barba-Espín G, Clemente-Moreno M, Hernández J. 2010. Characterization of the antioxidant system during the vegetative development of pea plants. *Biologia Plantarum* **54**, 76-82.

Dixon DP, Hawkins T, Hussey PJ, Edwards R. 2009a. Enzyme activities and subcellular localization of members of the Arabidopsis glutathione transferase superfamily. *Journal of Experimental Botany* **60**, 1207-1218.

Dixon DP, Skipsey M, Edwards R. 2010. Roles for glutathione transferases in plant secondary metabolism. *Phytochemistry* **71**, 338-350.

Dixon LB, Dickerson F, Bellack AS, Bennett M, Dickinson D, Goldberg RW, Lehman A, Tenhula WN, Calmes C, Pasillas RM. 2009b. The 2009 schizophrenia PORT psychosocial treatment recommendations and summary statements. *Schizophrenia Bulletin* **36**, 48-70.

Dron M, Lacasa M, Tovey M. 1990. Priming affects the activity of a specific region of the promoter of the human beta interferon gene. *Molecular and Cellular Biology* **10**, 854-858.

Droux M, Ruffet ML, Douce R, Job D. 1998. Interactions between serine acetyltransferase and O‐acetylserine (thiol) lyase in higher plants. *The FEBS Journal* **255**, 235-245.

Duruibe JO, Ogwuegbu M, Egwurugwu J. 2007. Heavy metal pollution and human biotoxic effects. *International Journal of Physical Sciences* **2**, 112-118.

Edwards R, Dixon DP. 2005. Plant glutathione transferases. *Methods in Enzymology* **401**, 169-186.

Ellis RJ, Macdonald IR. 1970. Specificity of Cycloheximide in Higher Plant Systems. *Plant Physiology* **46**, 227-+.

Farooq A, Zhou M-M. 2004. Structure and regulation of MAPK phosphatases. *Cellular Signalling* **16**, 769-779.

Feldman-Salit A, Wirtz M, Hell R, Wade RC. 2009. A mechanistic model of the cysteine synthase complex. *Journal of Molecular Biology* **386**, 37-59.

Felix G, Duran JD, Volko S, Boller T. 1999. Plants have a sensitive perception system for the most conserved domain of bacterial flagellin. *The Plant Journal* **18**,

265-276.

Fernandes AP, Holmgren A. 2004. Glutaredoxins: glutathione-dependent redox enzymes with functions far beyond a simple thioredoxin backup system. *Antioxidants and Redox Signaling* **6**, 63-74.

Ferretti M, Destro T, Tosatto S, La Rocca N, Rascio N, Masi A. 2009. Gamma-glutamyl transferase in the cell wall participates in extracellular glutathione salvage from the root apoplast. *New Phytologist* **181**, 115-126.

Foyer CH, Halliwell B. 1976. The presence of glutathione and glutathione reductase in chloroplasts: a proposed role in ascorbic acid metabolism. *Planta* **133**, 21-25.

Foyer CH, Noctor G. 2005. Redox homeostasis and antioxidant signaling: a metabolic interface between stress perception and physiological responses. *The Plant Cell* **17**, 1866-1875.

Foyer CH, Noctor G. 2011. Ascorbate and glutathione: the heart of the redox hub. *Plant Physiology* **155**, 2-18.

Foyer CH, Souriau N, Perret S, Lelandais M, Kunert K-J, Pruvost C, Jouanin L. 1995. Overexpression of glutathione reductase but not glutathione synthetase leads to increases in antioxidant capacity and resistance to photoinhibition in poplar trees. *Plant Physiology* **109**, 1047-1057.

Foyer CH, Theodoulou FL, Delrot S. 2001. The functions of inter-and intracellular glutathione transport systems in plants. *Trends in Plant Science* **6**, 486-492.

Fraser JA, Kansagra P, Kotecki C, Saunders RD, McLellan LI. 2003a. The modifier subunit of Drosophila glutamate-cysteine ligase regulates catalytic activity by covalent and noncovalent interactions and influences glutathione homeostasis in vivo. *Journal of Biological Chemistry* **278**, 46369-46377.

Fraser PA, Ding W-Z, Mohseni M, Treadwell EL, Dooley MA, St Clair EW, Gilkeson GS, Cooper GS. 2003b. Glutathione S-transferase M null homozygosity and risk of systemic lupus erythematosus associated with sun exposure: a possible gene-environment interaction for autoimmunity. *The Journal of Rheumatology* **30**, 276-282.

Frendo P, Jiménez MJH, Mathieu C, Duret L, Gallesi D, Van de Sype G, Hérouart D, Puppo A. 2001. A Medicago truncatula homoglutathione synthetase is derived from glutathione synthetase by gene duplication. *Plant Physiology* **126**, 1706-1715.

Frova C. 2003. The plant glutathione transferase gene family: genomic structure, functions, expression and evolution. *Physiologia Plantarum* **119**, 469-479.

Gadd GM. 2010. Metals, minerals and microbes: geomicrobiology and bioremediation.

Microbiology **156**, 609-643.

Gadjev I, Stone JM, Gechev TS. 2008. Programmed cell death in plants: new insights into redox regulation and the role of hydrogen peroxide. *International Review of Cell and Molecular Biology* **270**, 87-144.

Galant A, Preuss M, Cameron J, Jez J. 2011. Plant Glutathione Biosynthesis: Diversity in Biochemical Regulation and Reaction Products. *Frontiers in Plant Science* **2**.

Giles NM, Giles GI, Jacob C. 2003. Multiple roles of cysteine in biocatalysis. *Biochemical and Biophysical Research Communications* **300**, 1-4.

Giordano M, Raven JA. 2014. Nitrogen and sulfur assimilation in plants and algae. *Aquatic Botany* **118**, 45-61.

Giovanelli J. 1990. Regulatory aspects of cysteine and methionine biosynthesis. *Sulphur Nutrition and Sulphur Assimilation in Higher Plants*, 33-48.

Gogos A, Shapiro L. 2002. Large conformational changes in the catalytic cycle of glutathione synthase. *Structure* **10**, 1669-1676.

Grant CM. 2001. Role of the glutathione/glutaredoxin and thioredoxin systems in yeast growth and response to stress conditions. *Molecular Microbiology* **39**, 533-541.

Grant CM, MacIver FH, Dawes IW. 1997. Glutathione synthetase is dispensable for growth under both normal and oxidative stress conditions in the yeast Saccharomyces cerevisiae due to an accumulation of the dipeptide gamma-glutamylcysteine. *Molecular Biology of the Cell* **8**, 1699-1707.

Griffith OW, Meister A. 1979. Potent and specific inhibition of glutathione synthesis by buthionine sulfoximine (Sn-butyl homocysteine sulfoximine). *Journal of Biological Chemistry* **254**, 7558-7560.

Gromes R, Hothorn M, Lenherr ED, Rybin V, Scheffzek K, Rausch T. 2008. The redox switch of γ‐glutamylcysteine ligase via a reversible monomer–dimer transition is a mechanism unique to plants. *The Plant Journal* **54**, 1063-1075.

Grzam A, Martin MN, Hell R, Meyer AJ. 2007. γ‐Glutamyl transpeptidase GGT4 initiates vacuolar degradation of glutathione S‐conjugates in Arabidopsis. *FEBS Letters* **581**, 3131-3138.

Gunning J, Baron IZ. 2014. *Why occupy a square?: People, protests and movements in the Egyptian revolution*: Oxford University Press.

Gushima H, Yasuda S, Soeda E, Yokota M, Kondo M, Kimura A. 1984. Complete nucleotide sequence of the E. coli glutathione synthetase gsh-II. *Nucleic Acids Research* **12**, 9299-9307.

Hawkesford MJ. 2012. Sulfate uptake and assimilation–whole plant regulation. *Sulfur Metabolism in Plants*: Springer, 11-24.

Hell R, Bergmann L. 1990. λ-Glutamylcysteine synthetase in higher plants: catalytic properties and subcellular localization. *Planta* **180**, 603.

Hell R, Jost R, Berkowitz O, Wirtz M. 2002. Molecular and biochemical analysis of the enzymes of cysteine biosynthesis in the plant Arabidopsis thaliana. *Amino Acids* **22**, 245-257.

Herouart D, Van Montagu M, Inze D. 1993. Redox-activated expression of the cytosolic copper/zinc superoxide dismutase gene in Nicotiana. *Proceedings of the National Academy of Sciences* **90**, 3108-3112.

Herschbach C, Rennenberg H. 2001. Significance of phloem-translocated organic sulfur compounds for the regulation of sulfur nutrition. *Progress in Botany*: Springer, 177-193.

Hicks LM, Cahoon RE, Bonner ER, Rivard RS, Sheffield J, Jez JM. 2007. Thiol-based regulation of redox-active glutamate-cysteine ligase from Arabidopsis thaliana. *The Plant Cell* **19**, 2653-2661.

Hirata K, Tsuji N, Miyamoto K. 2005. Biosynthetic regulation of phytochelatins, heavy metal-binding peptides. *Journal of Bioscience and Bioengineering* **100**, 593-599.

Hothorn M, Bonneau F, Stier G, Greiner S, Scheffzek K. 2003. Expression, purification and crystallization of a thermostable tobacco invertase inhibitor. *Acta Crystallog. sect. D* **59**, 2279-2282.

Hothorn M, Wachter A, Gromes R, Stuwe T, Rausch T, Scheffzek K. 2006. Structural basis for the redox control of plant glutamate cysteine ligase. *Journal of Biological Chemistry* **281**, 27557-27565.

Howden R, Andersen CR, Goldsbrough PB, Cobbett CS. 1995. A cadmium-sensitive, glutathione-deficient mutant of Arabidopsis thaliana. *Plant Physiology* **107**, 1067-1073.

Jamai A, Tommasini R, Martinoia E, Delrot S. 1996. Characterization of glutathione uptake in broad bean leaf protoplasts. *Plant Physiology* **111**, 1145-1152.

Jez JM, Cahoon RE, Chen S. 2004. Arabidopsis thaliana Glutamate-Cysteine Ligase functional properties, kinetic mechanism, and regulation of activity. *Journal of Biological Chemistry* **279**, 33463-33470.

Jimenez A, Hernandez JA, del Río LA, Sevilla F. 1997. Evidence for the presence of the ascorbate-glutathione cycle in mitochondria and peroxisomes of pea leaves.

Plant Physiology **114**, 275-284.

Jiménez A, Hernández JA, Pastori G, del Rıo LA, Sevilla F. 1998. Role of the ascorbate-glutathione cycle of mitochondria and peroxisomes in the senescence of pea leaves. *Plant Physiology* **118**, 1327-1335.

Jonak C, Ökrész L, Bögre L, Hirt H. 2002. Complexity, cross talk and integration of plant MAP kinase signalling. *Current Opinion in Plant Biology* **5**, 415-424.

Kamata H, Honda S-i, Maeda S, Chang L, Hirata H, Karin M. 2005. Reactive oxygen species promote TNFα-induced death and sustained JNK activation by inhibiting MAP kinase phosphatases. *Cell* **120**, 649-661.

Kankipati HN, Rubio-Texeira M, Castermans D, Diallinas G, Thevelein JM. 2015. Sul1 and Sul2 sulfate transceptors signal to protein kinase A upon exit of sulfur starvation. *Journal of Biological Chemistry* **290**, 10430-10446.

Keillor JW, Castonguay R, Lherbet C. 2005. Gamma-glutamyl transpeptidase substrate specificity and catalytic mechanism. *Methods in Enzymology* **401**, 449-467.

Kerk D, Bulgrien J, Smith DW, Barsam B, Veretnik S, Gribskov M. 2002. The complement of protein phosphatase catalytic subunits encoded in the genome of Arabidopsis. *Plant Physiology* **129**, 908-925.

Keyse SM. 2000. Protein phosphatases and the regulation of mitogen-activated protein kinase signalling. *Current Opinion in Cell Biology* **12**, 186-192.

Keyse SM. 2008. Dual-specificity MAP kinase phosphatases (MKPs) and cancer. *Cancer and Metastasis Reviews* **27**, 253-261.

Kim HS, Ullevig SL, Zamora D, Lee CF, Asmis R. 2012. Redox regulation of MAPK phosphatase 1 controls monocyte migration and macrophage recruitment. *Proceedings of the National Academy of Sciences*, 201212596.

Klapheck S, Fliegner W, Zimmer I. 1994. Hydroxymethyl-phytochelatins [([gamma]-glutamylcysteine) n-serine] are metal-induced peptides of the poaceae. *Plant Physiology* **104**, 1325-1332.

Kouřil R, Lazar D, Lee H, Jo J, Nauš J. 2003. Moderately elevated temperature eliminates resistance of rice plants with enhanced expression of glutathione reductase to intensive photooxidative stress. *Photosynthetica* **41**, 571-578.

Kovtun Y, Chiu W-L, Tena G, Sheen J. 2000. Functional analysis of oxidative stress-activated mitogen-activated protein kinase cascade in plants. *Proceedings of the National Academy of Sciences* **97**, 2940-2945.

Krzywanski DM, Dickinson DA, Iles KE, Wigley AF, Franklin CC, Liu R-M, Kavanagh TJ, Forman HJ. 2004. Variable regulation of glutamate cysteine ligase

subunit proteins affects glutathione biosynthesis in response to oxidative stress. *Archives of Biochemistry and biophysics* **423**, 116-125.

Labrou NE, Papageorgiou AC, Pavli O, Flemetakis E. 2015. Plant GSTome: structure and functional role in xenome network and plant stress response. *Current Opinion in Biotechnology* **32**, 186-194.

Lallement P-A, Brouwer B, Keech O, Hecker A, Rouhier N. 2014. The still mysterious roles of cysteine-containing glutathione transferases in plants. *Frontiers in Pharmacology* **5**, 192.

Lee JS, Ellis BE. 2007. Arabidopsis MAPK phosphatase 2 (MKP2) positively regulates oxidative stress tolerance and inactivates the MPK3 and MPK6 MAPKs. *Journal of Biological Chemistry* **282**, 25020-25029.

Lee S, Leustek T. 1998. APS kinase fromArabidopsis thaliana: genomic organization, expression, and kinetic analysis of the recombinant enzyme. *Biochemical and Biophysical Research Communications* **247**, 171-175.

Leustek T, Martin MN, Bick J-A, Davies JP. 2000. Pathways and regulation of sulfur metabolism revealed through molecular and genetic studies. *Annual Review of Plant Biology* **51**, 141-165.

Leustek T, Saito K. 1999. Sulfate transport and assimilation in plants. *Plant Physiology* **120**, 637-644.

Lichten CA, Swain PS. 2011. A Bayesian method for inferring quantitative information from FRET data. *BMC Biophysics* **4**, 10.

Lillig CH, Schiffmann S, Berndt C, Berken A, Tischka R, Schwenn JD. 2001. Molecular and catalytic properties of Arabidopsis thaliana adenylyl sulfate (APS)-kinase. *Archives of Biochemistry and Bophysics* **392**, 303-310.

Liu X-M, Kim KE, Kim K-C, Nguyen XC, Han HJ, Jung MS, Kim HS, Kim SH, Park HC, Yun D-J. 2010. Cadmium activates Arabidopsis MPK3 and MPK6 via accumulation of reactive oxygen species. *Phytochemistry* **71**, 614-618.

Lu Y-P, Li Z-S, Drozdowicz YM, Hörtensteiner S, Martinoia E, Rea PA. 1998. AtMRP2, an Arabidopsis ATP binding cassette transporter able to transport glutathione S-conjugates and chlorophyll catabolites: functional comparisons with AtMRP1. *The Plant Cell* **10**, 267-282.

Lumbreras V, Vilela B, Irar S, Solé M, Capellades M, Valls M, Coca M, Pagès M. 2010. MAPK phosphatase MKP2 mediates disease responses in Arabidopsis and functionally interacts with MPK3 and MPK6. *The Plant Journal* **63**, 1017-1030.

Mailloux RJ, Jin X, Willmore WG. 2014. Redox regulation of mitochondrial function

with emphasis on cysteine oxidation reactions. *Redox Biology* **2**, 123-139.

Marinho HS, Real C, Cyrne L, Soares H, Antunes F. 2014. Hydrogen peroxide sensing, signaling and regulation of transcription factors. *Redox Biology* **2**, 535-562.

Marquet A, Bui BTS, Florentin D. 2001. Biosynthesis of biotin and lipoic acid. *Vitamins & Hormones* **61**, 51-101.

Marrs KA. 1996. The functions and regulation of glutathione S-transferases in plants. *Annual Review of Plant Biology* **47**, 127-158.

Martin MN, Slovin JP. 2000. Purified γ-Glutamyl Transpeptidases from Tomato Exhibit High Affinity for Glutathione and GlutathioneS-Conjugates. *Plant Physiology* **122**, 1417-1426.

Marty L, Siala W, Schwarzländer M, Fricker MD, Wirtz M, Sweetlove LJ, Meyer Y, Meyer AJ, Reichheld J-P, Hell R. 2009. The NADPH-dependent thioredoxin system constitutes a functional backup for cytosolic glutathione reductase in Arabidopsis. *Proceedings of the National Academy of Sciences* **106**, 9109-9114.

Matern S, Peskan-Berghoefer T, Gromes R, Kiesel RV, Rausch T. 2015. Imposed glutathione-mediated redox switch modulates the tobacco wound-induced protein kinase and salicylic acid-induced protein kinase activation state and impacts on defence against Pseudomonas syringae. *Journal of Experimental Botany* **66**, 1935-1950.

Maughan SC, Pasternak M, Cairns N, Kiddle G, Brach T, Jarvis R, Haas F, Nieuwland J, Lim B, Müller C. 2010. Plant homologs of the Plasmodium falciparum chloroquine-resistance transporter, PfCRT, are required for glutathione homeostasis and stress responses. *Proceedings of the National Academy of Sciences* **107**, 2331-2336.

May MJ, Leaver CJ. 1993. Oxidative stimulation of glutathione synthesis in Arabidopsis thaliana suspension cultures. *Plant Physiology* **103**, 621-627.

May MJ, Leaver CJ. 1994. Arabidopsis thaliana gamma-glutamylcysteine synthetase is structurally unrelated to mammalian, yeast, and Escherichia coli homologs. *Proceedings of the National Academy of Sciences* **91**, 10059-10063.

Mazid M, Khan T, Mohammad F. 2011. Role of secondary metabolites in defense mechanisms of plants. *Biology and Medicine* **3**, 232-249.

Meister A. 1995. [1] Glutathione metabolism. *Methods in Enzymology* **251**, 3-7.

Mendel RR, Hänsch R. 2002. Molybdoenzymes and molybdenum cofactor in plants. *Journal of Experimental Botany* **53**, 1689-1698.

Mendoza-Cózatl DG, Xie Q, Akmakjian GZ, Jobe TO, Patel A, Stacey MG, Song L,

Demoin DW, Jurisson SS, Stacey G. 2014. OPT3 is a component of the iron-signaling network between leaves and roots and misregulation of OPT3 leads to an over-accumulation of cadmium in seeds. *Molecular Plant* **7**, 1455-1469.

Messaritou G, Grammenoudi S, Skoulakis EM. 2009. Dimerization is essential for 14-3-3ζ stability and function in vivo. *Journal of Biological Chemistry*, jbc. M109. 045989.

Meyer AJ, Brach T, Marty L, Kreye S, Rouhier N, Jacquot JP, Hell R. 2007. Redox‐sensitive GFP in Arabidopsis thaliana is a quantitative biosensor for the redox potential of the cellular glutathione redox buffer. *The Plant Journal* **52**, 973-986.

Meyer AJ, Fricker MD. 2002. Control of demand-driven biosynthesis of glutathione in green Arabidopsis suspension culture cells. *Plant Physiology* **130**, 1927-1937.

Milla MAR, Maurer A, Huete AR, Gustafson JP. 2003. Glutathione peroxidase genes in Arabidopsis are ubiquitous and regulated by abiotic stresses through diverse signaling pathways. *The Plant Journal* **36**, 602-615.

Mittova V, Theodoulou FL, Kiddle G, Gómez L, Volokita M, Tal M, Foyer CH, Guy M. 2003. Coordinate induction of glutathione biosynthesis and glutathione‐metabolizing enzymes is correlated with salt tolerance in tomato. *FEBS Letters* **554**, 417-421.

Mizoguchi T, Ichimura K, Shinozaki K. 1997. Environmental stress response in plants: the role of mitogen-activated protein kinases. *Trends in Biotechnology* **15**, 15-19.

Mohan P, Barve M, Chatterjee A, Hosur RV. 2006. pH driven conformational dynamics and dimer‐to‐monomer transition in DLC8. *Protein Science* **15**, 335-342.

Mohan PK, Joshi MV, Hosur RV. 2009. Hierarchy in guanidine unfolding of DLC8 dimer: regulatory functional implications. *Biochimie* **91**, 401-407.

Møller IM. 2001. Plant mitochondria and oxidative stress: electron transport, NADPH turnover, and metabolism of reactive oxygen species. *Annual Review of Plant Biology* **52**, 561-591.

Moran JF, Iturbe-Ormaetxe I, Matamoros MA, Rubio MC, Clemente MR, Brewin NJ, Becana M. 2000. Glutathione and homoglutathione synthetases of legume nodules. Cloning, expression, and subcellular localization. *Plant Physiology* **124**, 1381-1392.

Mou Z, Fan W, Dong X. 2003. Inducers of plant systemic acquired resistance regulate NPR1 function through redox changes. *Cell* **113**, 935-944.

Mullineaux PM, Rausch T. 2005. Glutathione, photosynthesis and the redox

regulation of stress-responsive gene expression. *Photosynthesis Research* **86**, 459-474.

Nikiforova V, Bielecka M, Gakiere B, Krueger S, Rinder J, Kempa S, Morcuende R, Scheible W-R, Hesse H, Hoefgen R. 2006. Effect of sulfur availability on the integrity of amino acid biosynthesis in plants. *Amino Acids* **30**, 173-183.

Nikiforova VJ, Gakiere B, Kempa S, Adamik M, Willmitzer L, Hesse H, Hoefgen R. 2004. Towards dissecting nutrient metabolism in plants: a systems biology case study on sulphur metabolism. *Journal of Experimental Botany* **55**, 1861-1870.

Noctor G, Foyer CH. 1998. Ascorbate and glutathione: keeping active oxygen under control. *Annual Review of Plant Biology* **49**, 249-279.

Noctor G, Gomez L, Vanacker H, Foyer CH. 2002. Interactions between biosynthesis, compartmentation and transport in the control of glutathione homeostasis and signalling. *Journal of Experimental Botany* **53**, 1283-1304.

Noctor G, Mhamdi A, Chaouch S, Han Y, Neukermans J, Marquez‐Garcia B, Queval G, Foyer CH. 2012. Glutathione in plants: an integrated overview. *Plant, Cell & Environment* **35**, 454-484.

Nühse TS, Peck SC, Hirt H, Boller T. 2000. Microbial elicitors induce activation and dual phosphorylation of the Arabidopsis thaliana MAPK 6. *Journal of Biological Chemistry* **275**, 7521-7526.

Obrig TG, Culp WJ, McKeehan WL, Hardesty B. 1971. The mechanism by which cycloheximide and related glutarimide antibiotics inhibit peptide synthesis on reticulocyte ribosomes. *Journal of Biological Chemistry* **246**, 174-181.

Ohkama-Ohtsu N, Oikawa A, Zhao P, Xiang C, Saito K, Oliver DJ. 2008. A γ-glutamyl transpeptidase-independent pathway of glutathione catabolism to glutamate via 5-oxoproline in Arabidopsis. *Plant Physiology* **148**, 1603-1613.

Ohkama‐Ohtsu N, Zhao P, Xiang C, Oliver DJ. 2007. Glutathione conjugates in the vacuole are degraded by γ‐glutamyl transpeptidase GGT3 in Arabidopsis. *The Plant Journal* **49**, 878-888.

Ott M, Gogvadze V, Orrenius S, Zhivotovsky B. 2007. Mitochondria, oxidative stress and cell death. *Apoptosis* **12**, 913-922.

Palma JM, Jiménez A, Sandalio LM, Corpas FJ, Lundqvist M, Gomez M, Sevilla F, del Río LA. 2006. Antioxidative enzymes from chloroplasts, mitochondria, and peroxisomes during leaf senescence of nodulated pea plants. *Journal of Experimental Botany* **57**, 1747-1758.

Parisy V, Poinssot B, Owsianowski L, Buchala A, Glazebrook J, Mauch F. 2007.

Identification of PAD2 as a γ‐glutamylcysteine synthetase highlights the importance of glutathione in disease resistance of Arabidopsis. *The Plant Journal* **49**, 159-172.

Park J, Song WY, Ko D, Eom Y, Hansen TH, Schiller M, Lee TG, Martinoia E, Lee Y. 2012. The phytochelatin transporters AtABCC1 and AtABCC2 mediate tolerance to cadmium and mercury. *The Plant Journal* **69**, 278-288.

Pasternak M, Lim B, Wirtz M, Hell R, Cobbett CS, Meyer AJ. 2008. Restricting glutathione biosynthesis to the cytosol is sufficient for normal plant development. *The Plant Journal* **53**, 999-1012.

Pilon‐Smits EA, Zhu YL, Sears T, Terry N. 2000. Overexpression of glutathione reductase in Brassica juncea: effects on cadmium accumulation and tolerance. *Physiologia Plantarum* **110**, 455-460.

Pitzschke A, Schikora A, Hirt H. 2009. MAPK cascade signalling networks in plant defence. *Current Opinion in Plant Biology* **12**, 421-426.

Polekhina G, Board PG, Gali RR, Rossjohn J, Parker MW. 1999. Molecular basis of glutathione synthetase deficiency and a rare gene permutation event. *The EMBO Journal* **18**, 3204-3213.

Pomorski A, Kochańczyk T, Miłoch A, Krężel A. 2013. Method for accurate determination of dissociation constants of optical ratiometric systems: chemical probes, genetically encoded sensors, and interacting molecules. *Analytical Chemistry* **85**, 11479-11486.

Queval G, Jaillard D, Zechmann B, Noctor G. 2011. Increased intracellular H_2O_2 availability preferentially drives glutathione accumulation in vacuoles and chloroplasts. *Plant, Cell & Environment* **34**, 21-32.

Queval G, Thominet D, Vanacker H, Miginiac-Maslow M, Gakière B, Noctor G. 2009. H2O2-activated up-regulation of glutathione in Arabidopsis involves induction of genes encoding enzymes involved in cysteine synthesis in the chloroplast. *Molecular Plant* **2**, 344-356.

Rascio N, Navari-Izzo F. 2011. Heavy metal hyperaccumulating plants: how and why do they do it? And what makes them so interesting? *Plant Science* **180**, 169-181.

Reumann S, Corpas FJ. 2010. The peroxisomal ascorbate–glutathione pathway: molecular identification and insights into its essential role under environmental stress conditions. *Ascorbate-Glutathione Pathway and Stress Tolerance in Plants*: Springer, 387-404.

Riechers DE, Kreuz K, Zhang Q. 2010. Detoxification without intoxication: herbicide safeners activate plant defense gene expression. *Plant Physiology* **153**, 3-13.

Romeis T, Ludwig AA, Martin R, Jones JD. 2001. Calcium‐dependent protein kinases play an essential role in a plant defence response. *The EMBO Journal* **20**, 5556-5567.

Roos G, Messens J. 2011. Protein sulfenic acid formation: from cellular damage to redox regulation. *Free Radical Biology and Medicine* **51**, 314-326.

Rouached H, Secco D, Arpat AB. 2009. Getting the most sulfate from soil: regulation of sulfate uptake transporters in Arabidopsis. *Journal of Plant Physiology* **166**, 893-902.

Rouhier N, Lemaire SD, Jacquot J-P. 2008. The role of glutathione in photosynthetic organisms: emerging functions for glutaredoxins and glutathionylation. *Annu. Rev. Plant Biol.* **59**, 143-166.

Saito K. 2000. Regulation of sulfate transport and synthesis of sulfur-containing amino acids. *Current Opinion in Plant Biology* **3**, 188-195.

Samuel MA, Miles GP, Ellis BE. 2000. Ozone treatment rapidly activates MAP kinase signalling in plants. *The Plant Journal* **22**, 367-376.

Schlaeppi K, Bodenhausen N, Buchala A, Mauch F, Reymond P. 2008. The glutathione‐deficient mutant pad2‐1 accumulates lower amounts of glucosinolates and is more susceptible to the insect herbivore Spodoptera littoralis. *The Plant Journal* **55**, 774-786.

Schnaubelt D, Queval G, Dong Y, DIAZ‐VIVANCOS P, Makgopa ME, Howell G, De Simone A, Bai J, Hannah MA, Foyer CH. 2015. Low glutathione regulates gene expression and the redox potentials of the nucleus and cytosol in *Arabidopsis thaliana. Plant, Cell & Environment* **38**, 266-279.

Schneider A, Schatten T, Rennenberg H. 1994. Exchange between phloem and xylem during long distance transport of glutathione in spruce trees [Picea abies [Karst.] L. *Journal of Experimental Botany* **45**, 457-462.

Schürmann P, Buchanan BB. 2008. The ferredoxin/thioredoxin system of oxygenic photosynthesis. *Antioxidants & Redox Signaling* **10**, 1235-1274.

Schürmann P, Jacquot J-P. 2000. Plant thioredoxin systems revisited. *Annual review of Plant Bology* **51**, 371-400.

Setkov N, Kazakov V, Rosenwald I, Makarova G, Epifanova O. 1992. Protein synthesis inhibitors, like growth factors, may render resting 3T3 cells competent for DNA synthesis: a radioautographic and cell fusion study. *Cell Proliferation* **25**, 181-191.

Shaw ML, Pither-Joyce MD, McCallum JA. 2005. Purification and cloning of a

γ-glutamyl transpeptidase from onion (Allium cepa). *Phytochemistry* **66**, 515-522.

Shigeoka S, Ishikawa T, Tamoi M, Miyagawa Y, Takeda T, Yabuta Y, Yoshimura K. 2002. Regulation and function of ascorbate peroxidase isoenzymes. *Journal of Experimental Botany* **53**, 1305-1319.

Sies H, Berndt C, Jones DP. 2017. Oxidative stress. *Annual review of biochemistry* **86**, 715-748.

Signorelli S, Coitiño EL, Borsani O, Monza J. 2013. Molecular mechanisms for the reaction between •OH radicals and proline: insights on the role as reactive oxygen species scavenger in plant stress. *The Journal of Physical Chemistry B* **118**, 37-47.

Singla-Pareek SL, Yadav SK, Pareek A, Reddy M, Sopory S. 2006. Transgenic tobacco overexpressing glyoxalase pathway enzymes grow and set viable seeds in zinc-spiked soils. *Plant Physiology* **140**, 613-623.

Sobrino-Plata J, Meyssen D, Cuypers A, Escobar C, Hernández LE. 2014. Glutathione is a key antioxidant metabolite to cope with mercury and cadmium stress. *Plant and Soil* **377**, 369-381.

Song W-Y, Park J, Mendoza-Cózatl DG, Suter-Grotemeyer M, Shim D, Hörtensteiner S, Geisler M, Weder B, Rea PA, Rentsch D. 2010. Arsenic tolerance in Arabidopsis is mediated by two ABCC-type phytochelatin transporters. *Proceedings of the National Academy of Sciences* **107**, 21187-21192.

Srivastava S, D'souza S. 2009. Increasing sulfur supply enhances tolerance to arsenic and its accumulation in Hydrilla verticillata (Lf) Royle. *Environmental Science & Technology* **43**, 6308-6313.

Steinkamp R, Rennenberg H. 1985. Degradation of glutathione in plant cells: evidence against the participation of a γ-glutamyltranspeptidase. *Zeitschrift für Naturforschung C* **40**, 29-33.

Suzuki N, Suzuki T, Uchida A, Thompson EA, Hosoya T. 1992. Effect of dexamethasone on nucleolar casein kinase II activity and phosphorylation of nucleolin in lymphosarcoma P1798 cells. *The Journal of Steroid Biochemistry and Molecular Biology* **42**, 305-312.

Takahashi F, Mizoguchi T, Yoshida R, Ichimura K, Shinozaki K. 2011a. Calmodulin-dependent activation of MAP kinase for ROS homeostasis in *Arabidopsis*. *Molecular cell* **41**, 649-660.

Takahashi H, Kopriva S, Giordano M, Saito K, Hell R. 2011b. Sulfur assimilation in photosynthetic organisms: molecular functions and regulations of transporters and assimilatory enzymes. *Annual Review of Plant Biology* **62**, 157-184.

Toroser D, Sohal RS. 2005. Kinetic characteristics of native γ-glutamylcysteine ligase in the aging housefly, Musca domestica L. *Biochemical and Biophysical Research Communications* **326**, 586-593.

Toroser D, Yarian CS, Orr WC, Sohal RS. 2006. Mechanisms of γ-glutamylcysteine ligase regulation. *Biochimica et Biophysica Acta (BBA)-General Subjects* **1760**, 233-244.

Tu Z, Anders M. 1998. Expression and characterization of human glutamate–cysteine ligase. *Archives of Biochemistry and Biophysics* **354**, 247-254.

Vernoux T, Wilson RC, Seeley KA, Reichheld J-P, Muroy S, Brown S, Maughan SC, Cobbett CS, Van Montagu M, Inzé D. 2000. The ROOT MERISTEMLESS1/CADMIUM SENSITIVE2 gene defines a glutathione-dependent pathway involved in initiation and maintenance of cell division during postembryonic root development. *The Plant Cell* **12**, 97-109.

Vilela B, Pagès M, Lumbreras V. 2010. Regulation of MAPK signaling and cell death by MAPK phosphatase MKP2. *Plant Signaling & Behavior* **5**, 1497-1500.

Villiers F, Ducruix C, Hugouvieux V, Jarno N, Ezan E, Garin J, Junot C, Bourguignon J. 2011. Investigating the plant response to cadmium exposure by proteomic and metabolomic approaches. *Proteomics* **11**, 1650-1663.

Vivancos PD, Dong Y, Ziegler K, Markovic J, Pallardó FV, Pellny TK, Verrier PJ, Foyer CH. 2010a. Recruitment of glutathione into the nucleus during cell proliferation adjusts whole-cell redox homeostasis in Arabidopsis thaliana and lowers the oxidative defence shield. *The Plant Journal* **64**, 825-838.

Vivancos PD, Wolff T, Markovic J, Pallardó FV, Foyer CH. 2010b. A nuclear glutathione cycle within the cell cycle. *Biochemical Journal* **431**, 169-178.

Wachter A, Wolf S, Steininger H, Bogs J, Rausch T. 2005. Differential targeting of GSH1 and GSH2 is achieved by multiple transcription initiation: implications for the compartmentation of glutathione biosynthesis in the Brassicaceae. *The Plant Journal* **41**, 15-30.

Wei-Min S, HUANG Z-Z, Shelly CL. 1996. Regulation of γ-glutamylcysteine synthetase by protein phosphorylation. *Biochemical Journal* **320**, 321-328.

Willekens H, Chamnongpol S, Davey M, Schraudner M, Langebartels C, Van Montagu M, Inze D, Van Camp W. 1997. Catalase is a sink for H2O2 and is indispensable for stress defence in C3 plants. *The EMBO Journal* **16**, 4806-4816.

Wingate VP, Lawton MA, Lamb CJ. 1988. Glutathione causes a massive and selective induction of plant defense genes. *Plant Physiology* **87**, 206-210.

Wirtz M, Droux M. 2005. Synthesis of the sulfur amino acids: cysteine and methionine. *Photosynthesis Research* **86**, 345-362.

Wirtz M, Hell R. 2006. Functional analysis of the cysteine synthase protein complex from plants: structural, biochemical and regulatory properties. *Journal of Plant physiology* **163**, 273-286.

Wittstock U, Halkier BA. 2002. Glucosinolate research in the Arabidopsis era. *Trends in Plant Science* **7**, 263-270.

Wolf AE, Dietz KJ, Schröder P. 1996. Degradation of glutathione S-conjugates by a carboxypeptidase in the plant vacuole. *FEBS Letters* **384**, 31-34.

Wu JQ, Kosten TR, Zhang XY. 2013. Free radicals, antioxidant defense systems, and schizophrenia. *Progress in Neuro-Psychopharmacology and Biological Psychiatry* **46**, 200-206.

Xiang C, Oliver DJ. 1998. Glutathione metabolic genes coordinately respond to heavy metals and jasmonic acid in Arabidopsis. *The Plant Cell* **10**, 1539-1550.

Yadav S. 2010. Heavy metals toxicity in plants: an overview on the role of glutathione and phytochelatins in heavy metal stress tolerance of plants. *South African Journal of Botany* **76**, 167-179.

Yang YX, Lenherr ED, Gromes R, Wang SS, Wirtz M, Hell R, Scheffzek K, Rausch T. 2008. Regulation of plant glutamylcysteine ligase: Redox-mediated enzyme activation does not require homodimerization. *Submitted*

Yu M, Lamattina L, Spoel SH, Loake GJ. 2014. Nitric oxide function in plant biology: a redox cue in deconvolution. *New Phytologist* **202**, 1142-1156.

Zhang H, Forman HJ, Choi J. 2005. γ-Glutamyl Transpeptidase in Glutathione Biosynthesis. *Methods in Enzymology* **401**, 468-483.

Zhang X, Xu H, Dong Z, Wang Y, Liu J, Shen J. 2004. Highly efficient dendrimer-based mimic of glutathione peroxidase. *Journal of the American Chemical Society* **126**, 10556-10557.

Zhang ZY, Wang Y, Wu L, Fauman EB, Stuckey JA, Schubert HL, Saper MA, Dixon JE. 1994. The Cys (X) 5Arg catalytic motif in phosphoester hydrolysis. *Biochemistry* **33**, 15266-15270.

Zhang Z, Xie Q, Jobe TO, Kau AR, Wang C, Li Y, Qiu B, Wang Q, Mendoza-Cózatl DG, Schroeder JI. 2016. Identification of AtOPT4 as a plant glutathione transporter. *Molecular Plant* **9**, 481.

Zybailov B, Rutschow H, Friso G, Rudella A, Emanuelsson O, Sun Q, van Wijk KJ. 2008. Sorting signals, N-terminal modifications and abundance of the chloroplast

proteome. *PloS One* **3**, e1994.

9. Acknowledgements

Firstly, I would like to appreciate Prof. Dr. Thomas Rausch for giving me this precious opportunity to pursue my PhD study. I am very thankful for his guidance on my PhD project. His great support has benefited me a lot in academic research as well as in life.

I sincerely thank my second supervisor Prof. Dr. Rüdiger Hell for very helpful suggestions on my PhD project. Moreover, I deeply appreciate Prof. Dr. Luise Krauth-Siegel as a member of my Thesis Advisory Committee (TAC) and for giving me important scientific guidance.

I also thank the China Scholarship Council for providing scholarships for my PhD study. It is a great support for me to live abroad.

In addition, I have so appreciated the guidance from my colleague Tatjana Peskan-Berghöfer. I have learned from her about how to do the critical thinking in a more comprehensive way from designing experiments to interpreting the scientific results. I really thank Tatjana Peskan-Berghöfer, Katja Machemer-Noonan, Roland Gromes and Steffen Greiner for revising this thesis and for the research ideas they inspire me. Moreover, I sincerely appreciate Markus Wirtz, Shanshan Wang, Hongbin Wei, Hongbo Zhao, Yang Jiang, Wan Zhang, Feng He, Philippe Golfier, Heike Steininger and Cornelia Walter. they kindly provide me valuable advice from all aspects. And I thank Jeremy Sloan for experimental collaborations. I thank all the people who supported me during the PhD studies.

In the end, I would like to appreciate my families especially my parents for great accompany.